

University of Windsor

Scholarship at UWindor

Electronic Theses and Dissertations

Theses, Dissertations, and Major Papers

11-13-2018

CIR Parametric Rules Precocity For Ranging Error Mitigation In IR-UWB

Sunil K. Meghani
University of Windsor

Follow this and additional works at: <https://scholar.uwindsor.ca/etd>

Recommended Citation

Meghani, Sunil K., "CIR Parametric Rules Precocity For Ranging Error Mitigation In IR-UWB" (2018).
Electronic Theses and Dissertations. 7618.
<https://scholar.uwindsor.ca/etd/7618>

This online database contains the full-text of PhD dissertations and Masters' theses of University of Windsor students from 1954 forward. These documents are made available for personal study and research purposes only, in accordance with the Canadian Copyright Act and the Creative Commons license—CC BY-NC-ND (Attribution, Non-Commercial, No Derivative Works). Under this license, works must always be attributed to the copyright holder (original author), cannot be used for any commercial purposes, and may not be altered. Any other use would require the permission of the copyright holder. Students may inquire about withdrawing their dissertation and/or thesis from this database. For additional inquiries, please contact the repository administrator via email (scholarship@uwindsor.ca) or by telephone at 519-253-3000ext. 3208.

CIR Parametric Rules Precocity For Ranging Error Mitigation In IR-UWB

By

Sunil K. Meghani

A Thesis

Submitted to the Faculty of Graduate Studies
through the Department of Electrical and Computer Engineering
in Partial Fulfillment of the Requirements for
the Degree of Doctor of Philosophy at the
University of Windsor

Windsor, Ontario, Canada

2018

© 2018 Sunil Kumar Meghani

CIR Parametric Rules Precocity For Ranging Error Mitigation In IR-UWB

By
Sunil K. Meghani
Approved by:

J. Poncela, External Examiner
University of Malaga, Spain

R. Carriveau
Department of Mechanical, Automotive & Materials Engineering

M. Khalid
Department of Electrical & Computer Engineering

E. Abdel-Raheem
Department of Electrical & Computer Engineering

K. Tepe, Advisor
Department of Electrical & Computer Engineering

November 13, 2018

DECLARATION OF CO-AUTHORSHIP/ PREVIOUS PUBLICATION

I. Co-Authorship

I hereby declare that this dissertation incorporates some materials part of which are results of joint researches. The investigations and evaluations done throughout this dissertation used some technologies that were developed in the WiCIP research laboratory. The investigations were supported by collaborative help from my colleagues in WiCIP lab in the form of advice, critiques, mentoring, and teamwork. This dissertation also incorporates the outcome of joint research undertaken with Mati, Tank, and Marquez under the supervision of Professor Dr. Kemal Tepe. In addition, Muhammad Asif and Farooq Awin contributed technical knowledge and facilitated research work. In all cases, the key ideas, primary contributions, experimental designs, data analysis, and interpretation, were performed by the author, and the contribution of co-authors was primarily through the provision of suggestions, comments, critiques, verification, and other supports. I am aware of the University of Windsor Senate Policy on Authorship and certify that I have properly acknowledged the contribution of other researchers to my dissertation, and have obtained written permission from each of the co-author(s) to include the above material(s) in my dissertation.

II. Previous Publication

This dissertation includes three original papers that have been previously published/submitted for publication in peer-reviewed journals and conferences as follows:

Dissertation chapter	Publication title/full citation	Status
Part of Chapter 3 and 5	S.K. Meghani, M. Asif, F. Awin, K. Tepe; “Empirical Based Ranging Error Mitigation in IR-UWB: A Fuzzy Approach”	Submitted
Part of chapter 3 and 5	A. Marquez, B. Tank, S. K. Meghani, S. Ahmed, K. Tepe; “Accurate UWB and IMU based indoor localization for autonomous robots” presented at IEEE 30th Canadian Conference on Electrical and Computer Engineering (CCECE) Canada-2017	Published
Part of chapter 3 and 4	M. Mati, K. Tepe, S.K. Meghani; “Received Signal Strength Based NLOS Classification & Mitigation in Ultra Wide Band Localization System” presented at GC-WOC 2017	Published

I certify that I have obtained written permission from the copyright owner(s) to include the above-published material(s) in my dissertation. I certify that the above material describes work completed during my registration as a graduate student at the University of Windsor.

I declare that, to the best of my knowledge, my dissertation does not infringe upon anyone copyright nor violate any proprietary rights and that any ideas, techniques, quotations, or any other material from the work of other people included in my dissertation, published or otherwise, are fully acknowledged in accordance with the standard referencing practices. Furthermore, to the extent of that I have included copyrighted material that surpasses the bounds of fair dealing within the meaning of Canada Copyright Act, I certify that I have obtained written permission from copyright owner(s) to include such material(s) in my dissertation. I declare that this is a true copy of my dissertation, including any final revisions, as approved by my dissertation committee and the Graduate Studies office and that this dissertation has not been submitted for a higher degree to any other University or Institute.

ABSTRACT

The cutting-edge technology to support high ranging accuracy within the indoor environment is Impulse Radio Ultra Wide Band (IR-UWB) standard. Besides accuracy, IR-UWB's low-complex architecture and low power consumption align well with mobile devices. A prime challenge in indoor IR-UWB based localization is to achieve a position accuracy under non-line-of-sight (NLOS) and multipath propagation (MPP) conditions. Another challenge is to achieve acceptable accuracy in the conditions mentioned above without any significant increase in latency and computational burden. This dissertation proposes a solution for addressing the accuracy and reliability problem of indoor localization system satisfying acceptable delay or computational complexity overhead. The proposed methodology is based on rules for identification of line-of-sight (LOS) and NLOS and the range error bias estimation and correction due to NLOS and MPP conditions. The proposed methodology provides accuracy for two major application domains, namely, wireless sensor networks (WSNs) and indoor tracking and navigation (ITN). This dissertation offers two different solutions for the localization problem. The first solution is a rules-based classification of LOS / NLOS and geometric-based range correction for WSN. In the first solution, the Boolean logic based classification is designed for identification of LOS/NLOS. The logic is based on channel impulse response (CIR) parameters.

The second solution is based on fuzzy logic. The fuzzy based solution is appealing well for the stringent precision requirements in ITN. In this solution, the parametric Boolean logic from the first solution is converted and expanded into rules. These rules are implemented into a fuzzy logic based mechanism for designing a fuzzy inference system. The system estimates the ranging errors and correcting unmitigated ranges. The expanded rules and designed methodology are based on theoretical analysis and empirical observations of the parameters. The rules accommodate the parameters uncertainties for estimating the ranging error through the relationship between the input parameters uncertainties and ranging error using fuzzy inference mechanism.

The proposed solutions are evaluated using real-world measurements in different indoor environments. The performance of the proposed solutions is also evaluated in terms of true classification rate, residual ranging errors' cumulative distributions and probability density distributions, as well as outage probabilities. Evaluation results show that the true classification

rate is more than 95%. Moreover, using the proposed fuzzy logic based solution, the residual errors convergence of 90% is attained for error threshold of 10 cm, and the reliability of the localization system is also more than 90% for error threshold of 15 cm.

to my
Mother and Father
With love

ACKNOWLEDGMENTS

I would like to thank my advisor Dr. Kemal Tepe for introducing me into the research area of indoor localization, for his help and support during all phases of this dissertation and mainly for the many fruitful discussions, which always inspired and motivated me. I am grateful for all the time he dedicated to me and my work although he has many other students they also need his support. He became a good friend and I hope this relationship will last after the end of this study period too.

I would like to thanks my past colleague and friend Dr. Muhammad Asif and I feel special gratitude for all the time he dedicated and his advises to me and my work despite the long geographic distance between us.

I had many helpful and interesting discussions with all the other research group at WiCIP lab for their advice and enlightening discussions.

TABLE OF CONTENTS

	Page
Declaration of Co-Authorship/ Previous Publication	iii
Abstract	v
Dedication	vii
Acknowledgments	viii
List of Tables	xiii
List of Figures	xiv
List of Abbreviations	xv
1. Introduction	1
1.1. Introduction.....	1
1.2. Applications of indoor localization (IL)	1
1.3. Challenges in IL	2
1.4. Problem of Statement	4
1.5. Contributions	5
1.6. Research methodology	6
1.7. Dissertation organization	8
2. Background and Literature Review	9
2.1. Introduction	9
2.2. IL Positioning metrics	9
2.3. Types of ranging	10
2.3.1. Received signal strength indicator	10
2.3.2. Time of arrival	11
2.3.3. Time difference of arrival	11
2.4. Wireless standards used for IL	11
2.4.1. Impulse radio ultra wide band (IR-UWB)	11
2.4.2. Wireless local area network (WLAN)	12
2.4.3. Zigbee	12
2.4.4. Bluetooth	12

2.5. IR-UWB and IL	13
2.6. Positioning algorithm types	13
2.6.1. Least square trilateration	14
2.6.2. Extended Kalman filter (EKF)	14
2.6.3. Particle filter (PF)	15
2.7. Non-line-of-sight (NLOS) ranging error mitigation types	16
2.7.1. Range statistic based	17
2.7.2. CIR data based	17
2.7.3. Machine learning based	18
2.7.4. Fuzzy mapping based obstruction identification	19
2.8. Summary	19
3. Experimental studies	20
3.1. Introduction	20
3.2. Device selection for experiments	20
3.2.1. Comparison of Decawave and Time Domain devices	20
3.2.2. Decawave EVK-1000 kit description	21
3.3. Scenarios for experimental setups	24
3.3.1. Office scenarios.....	24
3.3.2. Warehouse Scenario.....	25
3.4. Observations of parameters in different scenarios	25
3.4.1. Received signal strength	25
3.4.2. First path signal strength	26
3.4.3. Rise time	27
3.4.4. Average CIR normalized magnitude	28
3.4.5. Leading edge normalized magnitude	29
3.4.6. First path max normalized magnitude	29
3.5. Summary	30
4. A parametric rule-based classification and localization algorithm for IR-UWB	31
4.1. Introduction	31
4.2. Classification of LOS and NLOS	32
4.2.1. Salient features in LOS and NLOS	32

4.2.2. Classification methodology	33
4.3. Range mitigation methodology	34
4.4. Experimental data	38
4.5. Results and discussions	38
4.5.1. Classification performance	38
4.5.2. Range mitigation performance	41
4.5.3. Localization performance	41
4.6. Summary.....	43
5. Rule based ranging error mitigation for IR-UWB: A fuzzy logic approach	45
5.1. Introduction	45
5.2. Fuzzy terminologies	46
5.2.1. Fuzzy set	46
5.2.2. Membership function	47
5.2.3. Fuzzification	47
5.2.4. Fuzzy inference	47
5.2.5. Defuzzification.....	48
5.3. Parameters uncertainty analysis	48
5.3.1. Received signal strength	48
5.3.2. First path signal strength	50
5.3.3. Rise time	50
5.3.4. Ranging error	51
5.4. Fuzzy inference system model	52
5.5. Experimental Evaluation.....	53
5.5.1. Experimental parameters analysis	54
5.5.2. Ranging error mitigation performance	55
5.5.3. Localization performance	59
5.6. Summary	61
6. Conclusion	62
6.1. Contributions	62
6.2. Future research directions	63
References	64

Appendix A: Copyright permission	69
Vita Auctoris	76

LIST OF TABLES

Page

2.1 Existing studies for classification and mitigating NLOS ranging errors in IR-UWB	16
3.1 Key characteristics of EVK-1000 & PulseON 410 kits.....	21
3.2: DW1000 operating characteristics.....	22
3.3 Scenarios and obstructions.....	24
4.1 Parameters observations in LOS and NLOS.....	32
4.2 Identification Rules for LOS/NLOS.....	33
4.3 Confusion Matrix.....	39
4.4 Range mitigated & NLOS Performance.....	41
5.1 Rules for FIS.....	55
5.2 Computational time	58

LIST OF FIGURES

Page

2.1 Different Methods for estimating leading edge based on energy detection	10
2.2 Ranging error variation in LOS and NLOS conditions	15
3.1 EVK-1000 kit EVB-1000 nodes	21
3.2 Mode of Operation of EVK-1000 Standalone vs. USB connection	22
3.3 Office floor plan	25
3.4 Warehouse floor plan	26
3.5 Parameters PDF in different scenarios	27
3.6 Average magnitude (M_{AVG}), FP-Min (M_{LEP}), and FP-Max (M_{FPM}) levels in different scenarios	28
4.1 Anchors and agent nodes placement	35
4.2 Flow-chart of the proposed algorithm	37
4.3 Performance comparison of different classifiers	40
4.4 Localization performance	42
4.5 Histogram & CDF of NLOS & Mitigated Algorithm ranges	43
5.1 Fuzzy classification & membership function	46
5.2 Rules structure	48
5.3 RSS and LOS/NLOS	49
5.4 CIR in LOS and NLOS	50
5.5 FIS Model	52
5.6 Inputs & outputs MFs for FIS model	54
5.7 Performance evaluation for different MFs and defuzzification processes	56
5.8 CDF for residual ranging errors.....	57
5.9 Anchors Placement around Target node with different d_i according to (5.22)	58
5.10 Outage Probability for various N_a with varying P_{NLOS}	59
5.11 Outage Probability for $N_a = 3$ with varying P_{NLOS} in worst scenarios	60

LIST OF ABBREVIATIONS

AN	Anchor Node
A_i	i^{th} AN placement
BEKF	Biased extended Kalman filter
CIR	Channel impulse response
CDF	cumulative distribution function
$d_{Mitigated}$	Mitigated distance
d_{NLOS}	NLOS distance
EKF	Extended Kalman filter
ε_{Mit}	Percentage error
EU ETSI EN	European Union European Telecommunications Standards Institute European Standard
FCC	Federal Communications Commission
F_1	Leading edge MPC
F_2	Second MPC in the first path after F_1
F_3	Third MPC in the first path after F_1
F_s	Strongest MPC in CIR
FIS	Fuzzy inference system
FP	False positive
FPSS	First path signal strength
FPR	False positive rate
FN	False negative
FNR	False negative rate
GNSS	Global navigation satellite system
GoC	Centre of gravity
GPS	Global positioning system

HM	Height method
IL	Indoor localization
ITN	Indoor tracking and navigation
IR-UWB	Impulse radio ultra wide band
K	Proportionality constant
KF	Kalman filter
LED	Leading edge detection
LOS	line-of-sight
LS-SVM	Least square support vector machine
M_{AVG}	Average CIR normalized magnitude
M_{LEP}	Leading edge normalized
M_{FPM}	First path max normalized magnitude
MEMS	Microelectronic mechanical system
MF	Membership function
MISO	Multiple input single output
MoM	Mean of maximum
MPC	Multipath component
MPP	Multipath propagation
MWSN	Mobile WSN
N	Number of measurements
N_a	Number of anchor nodes
NLOS	non-line-of-sight
PA	Position algorithm
PDF	probability density function
PF	Particle filter
PIF	Position improvement factor
P_{NLOS}	Probability of NLOS

P_{out}	Outage probability
PSD	Power spectral density
P_T	Misclassification rate
RRE	Residual range error
RSS	Received signal strength
RSSI	Received signal strength indicator
RMS	Root mean square
$R_{Mit.}$	Mitigated range
$R_{true.}$	True range
RT	Rise time
RTLS	Real-time localization system
RTtoA	Round trip time of arrival
RX	Receiver
SNLOS	Soft NLOS
SNR	Signal to noise ration
SPI	Serial peripheral interface
SVDD	Support vector data description
TD	Time difference
TDtoA	Time difference of arrival
T_{IN-OUT}	Input-output delay time
TN	Target node
TN_a	True negative
TP	True positive
ToA	Time of arrival
TDMA	Time division multiple access
TOF	Time of flight
TSK	Takagi-Sugeno-Kang

TW-ToA	Two way time of arrival
TX	Transmitter
WLAN	Wireless local area network
WSN	Wireless sensor network
2D	Two dimensional
δ_{imp}	range improvement factor
μ	Constant
β	Constant

1.1. Introduction

Locating position and navigating routes in indoors where global navigation satellite systems' (GNSS) signals cannot penetrate fall under indoor localization (IL) (or indoor positioning). IL has been gaining attention from the research community and industry in recent years due to widespread applications requiring either standalone or in conjunction with data communication where GNSS ceases to perform [13-15]. In IL, there are two types of nodes namely target node (TN) and anchor node (AN). The TN needs to be localized, and the AN is at a known position. The localization requires two phases, i.e., (i) ranging and (ii) positioning. In the ranging process, the distance between TN and AN(s) is estimated. The estimated distance utilizes radio signal characteristics such as received signal strength and received signal timing information. In the positioning phase, usually more than one estimated distances or one estimated distance in addition to an estimated angle of arrival of the ranging signals are used to determine the agent's position.

Ranging in IL under non-line-of-sight (NLOS) and multipath propagation (MPP) conditions is a challenging task is due to estimation of errors caused by obstructed and blocked, scattered, diffracted and reflected signals. The indoor environment exhibits dense multipath channel due to metal objects in the vicinity; usually found on factory and building floors and walls. In these environments impulse radio ultra-wide-band (IR-UWB) is the optimum choice for providing sub-centimeter positioning accuracy [6, 16]. However, NLOS is still a most critical challenge in IR-UWB for achieving that accuracy [17, 18].

1.2. Applications of IL

In this section, application domains that require IL as standalone or as an add-on to enhance functionality, operability, and capability of the domain and stretch domain's applicability in applications are discussed. Those domains are as follows:

- **Robots & Drones**

In recent years, besides stationary robots are used extensively in traditional industrial applications, drones, as well as mobile robots, find a way in a range of applications which

Chapter 1

span from industrial floors, smart warehouses, surveillance, military, civil engineering, domestic applications and many innovative applications [15, 17]. For instance, drones are used in [19] for site monitoring and [20] for indoor rescue service. For all these applications, IL is the fundamental technology which supports finding routes and navigating around from one place to another.

- **Wireless Sensor Network (WSN)**

In the past two decades, WSN flourished and developed at an exponential rate due to advancement and mass scale developments in micro-electromechanical system (MEMS), fabricated chip systems and wireless communication [21]. These technologies are integrated on a platform called sensor nodes. The nodes measure parameters (e.g., temperature and pressure), process data and store it. The interconnections of these nodes formed a network called WSN. Due to the added value to the number of systems, WSN finds a way in many applications in civil and military domains [22]. In the application domains, WSN functionality and applicability are significantly enhanced with localization. For instance, WSN's routing capability and energy consumption can be optimized through geographical information based routing protocols [22]. Also, localization plays a central role in mobile WSN (MWSN). In most of the WSN applications, IL is the best fit for WSN [21].

1.3. Challenges in IL

- **NLOS & Multipath**

IL is operated in indoor and cluttered environments. In these conditions, signal propagation experienced reflection, refraction diffraction and shadowing due to which signal arrived at the receiver in multiple paths called multipath propagation [23]. Also, the direct signal path from transmitter and receiver (known as line-of-sight path) is partially or fully blocked due objects in the vicinity. The blocked propagation is known as NLOS. Both Multipath and NLOS occur frequently and impact the ranging estimation error, which in turn degrades position accuracy significantly [18, 24].

- **Latency**

Chapter 1

Latency in estimating the position of the TN occurs at both phases (i.e., ranging and positioning). In the ranging phase, latency depends on the employed spectrum and data rates, technique to estimate distance (i.e., time-of-arrival), and propagation condition. Mainly, the NLOS propagation condition introduces a significant delay in estimating range error bias and correcting ranging where statistically based solutions employed due to the required number of measurements [25, 26]. In the positioning phase, delay depends on the algorithm that is used and the number of ANs that are participating in positioning. For instance, in the trilateration algorithm, increasing ANs beyond the minimum requirement (i.e., three ANs) increases position accuracy [27].

- **Computational Cost**

Computational complexity, hence its cost, depends on the employed wireless standard, ranging technique, position algorithm, and propagation condition. In case of wireless standard, IR-UWB considered being low complex in hardware implementation [28, 29]. For ranging technique, received signal strength (RSS) based estimation is less complex than other techniques stated in [30], and RSS is available in many wireless standards [31-33]. For positioning algorithm, a particle filter (PF) algorithm is the least computationally efficient among the available algorithms [34, 35].

- **Energy [36]**

Energy is a primary concern for mobile devices since these devices have limited power sources. Enhancing position accuracy requires more use of detection techniques, more sophisticated positioning algorithms (i.e., requires more computational resources) and more radio sensing which aggravated energy usage. That is why a trade-off between energy requirement and location accuracy needs to be established.

- **Interference**

Indoor communication is done mostly in the unlicensed spectrum such as wireless local area network (WLAN), IR-UWB, and Zigbee. Due to this, signal interference from the adjacent band and other sources degrade the performance of the system [37]. Although IR-UWB designed provides immunity from different wireless standards regarding interference

Chapter 1

[38], but interference within the spectrum due to adjacent signals pose a challenge in the reliable operation.

- **Security & Privacy [22]**

Location information and access to the localization system should provide security features and controlled access. Lack of these features makes system susceptible to malicious activities that can falsely advertise locations, altered routes, and degrade or halt the system functioning. Moreover, in mission-critical applications (e.g., in the military domain), the location information should be secured with enhanced security features.

- **Scalability[33]**

Scalable positioning system ensures normal positioning function as positioning scope expands. The expansion can be in terms of the increased number of requests for localization or geographical coverage. A scalable system in the sense of capacity wise is one that can handle the localization requests within specified requirements without any interruption in services. Regarding geographical coverage, a scalable system is one that ensures interrupted services as the system switches localization requests between the ANs. Usually, a positioning system with limited ANs covers a specific area. As the distance between the AN(s) and TN increases, location accuracy performance decreases. So to expand the coverage, more ANs are added.

1.4. Problem Statement

In this dissertation, solutions to the problems associated with NLOS and multipath propagations that impact position accuracy, position updates, and computational burden of real-time IL systems for tracking and navigation based on the IR-UWB spectrum are investigated. Solutions to the following specific problems are investigated:

Problem 1. Position Accuracy: Due to NLOS and multipath conditions, ranging error bias is induced in the ranging estimation between AN and TN. The estimated ranges are used in position algorithms to determine TN position. Due to the error, TN's location gets corrupted, and position accuracy affected.

Chapter 1

Problem 2. Position Updates: In order to compensate ranging error, multiple measurements are required to obtain statistics of the error to mitigate it. These measurements induce latency and affect position updates. Furthermore, acquisition of channel impulse response (CIR) whole frame data for the parameters estimation can induce further delay for particular measurement [1].

Problem 3. Computational Complexity: Additional processing is required to mitigate ranging errors due to NLOS. So, solutions which are computational intensive add additional computational burden and complexity. For example, the machine learning solutions which estimate range error bias under NLOS conditions [3] and particle filter (PF) for estimating position while reducing ranging errors [39].

1.5. Contributions

The main contributions of this dissertation are:

1. A novel rule-based classification of line-of-sight (LOS) and NLOS channel condition is proposed, and performance of this classifier is evaluated using empirical data and compared with existing works in [7, 40]. The rules are designed using empirical analysis of the collected channel impulse responses (CIRs) in different environments. The rules utilize CIR's parameters such as received signal strength (RSS), first path signal strength (FPSS) and rise time (RT) which are readily available from Decawave® devices and doesn't incur an additional delay in estimating the conditions. Moreover, the geometric correction of one range (which is NLOS range) out of three ranges algorithm is presented. This is suitable for applications such as WSN where one out of three AN-TN pairs is most likely experience NLOS condition at a particular location. The assumption is supported with Probabilistic Model.
2. A novel fuzzy logic based range error mitigation under LOS and NLOS conditions solution is proposed and evaluated using residual range error (RRE) cumulative density function (CDF) and localization outage probability (P_{out}) metrics. The rules for the classification are further expanded to estimate range error bias in LOS and NLOS conditions using the parameters. Moreover, the range bias error is estimated in one step rather than in two steps namely identification of LOS/NLOS condition and mitigation of ranging errors. First, the

Chapter 1

correlation between ranging error and the parameters under different channel conditions is developed. Second, the correlation is utilized as an expert knowledge for a fuzzy mechanism to design rules for fuzzy inference. The work is compared with work from [12] in terms of RRE CDF delay in estimating the error. Moreover, the proposed fuzzy based system is also compared with [12] for computational complexity in terms of input-output delay time [41]. The proposed solution shows a promising performance and reduces delay in estimating ranging error bias compared to [12]. Moreover, the proposed system doesn't require any training phase prior to estimating the error as it is validated in different environments.

The results show that the proposed rule-based solutions exhibit the following desired properties closely: enhanced localization accuracy under MPP and NLOS conditions, enhanced positioning availability under NLOS conditions, and reduced computational burden. While providing those benefits, it doesn't add latency in estimating range error bias.

1.6. Research Methodology

All problems discussed in 1.5 related to range error bias estimation and correction are addressed in this dissertation. In this work, uncertainties in the CIR's parameters due to NLOS and MPP conditions and its correlation to range error bias are analyzed through the extensive experimental campaign. It is found that designing rule based on the correlation is acceptable in an implementation using fuzzy inference mechanism for estimating the error bias. Therefore, the following methodological steps are performed:

Step#1. Measurements: In this phase, extensive experimental studies are done in three different environments. The experiments are conducted using Decawave® devices, and different NLOS scenarios are emulated in real-time using different obstructions. In each scenario, CIRs are collected along with other parameters.

Step#2. Analysis: Extensive analysis is done on measured parameters to understand the variation of different parameters in different channel conditions. The relationship between measured parameters and ranging errors is also analyzed.

Step#3. Rules Development: Rules have developed at this stage to classify the condition (i.e., LOS and NLOS). The rules are established using a comparison mechanism in which the parameters

Chapter 1

are compared with predefined thresholds. The thresholds are derived through empirical analysis done in the previous step.

Step#4. Expanding rules & Regression: In this phase, rules are further expanded to identify errors in LOS and NLOS. The mapping between the parameters (inputs) and range error bias (output) is developed through the expanded rules. The mapping is realized through theoretical and empirical analysis of parameters uncertainties and their correlation with the error bias.

Step#5. Applying Fuzzy Logic: The discrete rules developed in the preceding step are implemented using a fuzzy mechanism to estimate the error bias in a continuous way. Moreover, measurements uncertainty are covered optimally by the fuzzy approach. The uncertainties in the parameters are induced due to NLOS and MPP.

Chapter 1

1.7. Dissertation Organization

A background and literature review is given in Chapter 2. Chapter 3 discusses the devices selected for experiments and describes the scenarios' setup as well as analyze parameters' variations in different scenarios. Chapter 4 describes the methodology of rule-based classification of LOS and NLOS and geometric range correction. Chapter 5 presents a detailed design methodology of Fuzzy logic based ranging error mitigation and performance evaluation. In Chapter 6, the conclusions of the proposed research in this dissertation is summarized, and some recommendations for future work are presented.

BACKGROUND & LITERATURE REVIEW

2.1. Introduction

The process of estimating the distance between TN and AN is called ranging. Electronically, ranging process is done with the help of signal transmission between the nodes which are acted as transmitter and receiver through signal properties (i.e., timing, received power level or phase information). Ranging with accuracy is critical for estimating the position of TN close to the TN's true position and reliable performance of IL. Moreover, accurate ranging in IL is not a trivial task because of prevailing MPP and NLOS conditions in indoor and RF harsh environments. Notably, these conditions are dynamically changed for moving TN. Therefore, techniques are needed that can estimate and correct ranging error from signal properties due to the conditions. Moreover, the techniques that enhance accuracy and hence reliability have various influences on IL's availability, latency, computational requirement, and energy consumption [33].

In this chapter, first, metrics used in this research that gauge and impact the positioning performance are discussed. Second, types of ranging and wireless standards used in IL are reviewed. Third, the advantages of IR-UWB standard for precision localization are discussed. Fourth, review of existing positioning algorithms which are used specifically in IR-UWB are presented. Fifth, existing studies of NLOS (or LOS) classification and ranging error mitigation based on IR-UWB are reviewed. Also, their advantages and shortcomings are discussed. Finally, the chapter is summarized in the Summary section.

2.2. IL Positioning Metrics

The positioning metrics are used to express various objectives of the positioning with respect to the reliable functioning of IL. This section provides a brief overview of the positioning metrics related to this study:

- A. Accuracy: Accuracy is defined as how close the estimated position of TN to TN's true position. Therefore, accurate IL system is that in which difference between the estimated

Chapter 2

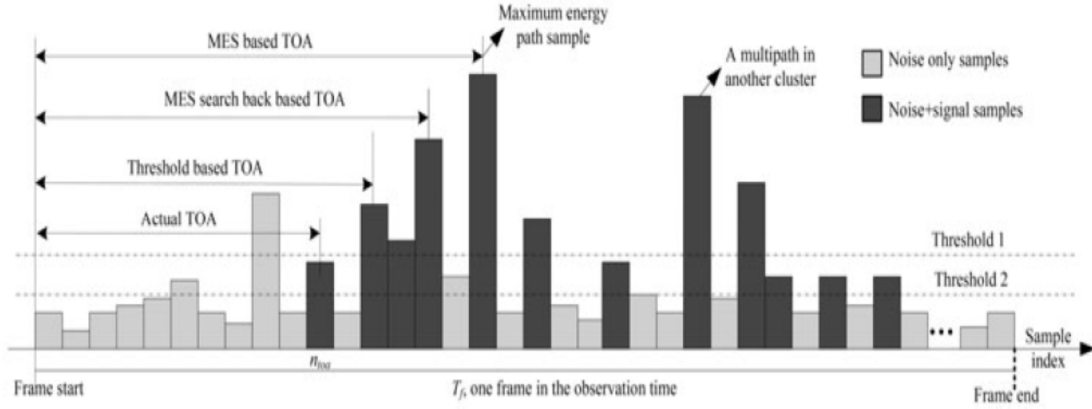


Fig. 2.1: Different Methods for estimating leading edge based on energy detection [4].

position and the true position should be minimum under all operating conditions. Thus, it is crucial to minimize ranging errors and others errors that affect positioning accuracy.

- B. Availability: It is defined as for specific operating (error) threshold, the localization system is available for the percentage of time available under different operating conditions. The metric shows the robustness against different errors for tolerable threshold error.
- C. Latency: It is defined as a delay in estimating TN position provided a request is made for the estimation. For fast positioning updates, delay in ranging acquisition, estimating ranging error and mitigating the error, and estimating positions from ranges are taken into consideration and should be minimized.

2.3. Types of Ranging

In this section, an overview of different ranging techniques and their pros and cons are discussed. The techniques are based on received signal and timing information of the signal and are as follows.

2.3.1. Received Signal Strength Indicator (RSSI)

RSSI is the most commonly used ranging estimation technique in wireless localization systems [42-44] because it is readily available in the form of received power strength. The estimation process is based on the Friis equation [45] using transmitted and received powers. However, RSSI based ranging and positioning performance degrades significantly under NLOS conditions due to

Chapter 2

attenuation of received signals related to obstruction between the transmitter (TX) and receiver (RX) [46].

2.3.2. Time Of Arrival (ToA)

In ToA, ranging is estimated using signal arrival time after synchronization between TX and RX. Usually, detection of the arrival time is implemented using a threshold based edge detection method [1, 47]. In the literature, different methods are suggested for detecting leading edge after the threshold as illustrated in Fig. 1. The setting of the threshold and detection mechanism affects the ranging performance in LOS and NLOS conditions [4, 47, 48]. From the arrival time, the propagation time between TX and RX is obtained, and thus distance is estimated using RF signal speed (i.e., the speed of light). In ToA, precision synchronization between TX and RX is required [49]. However, variation to TOA which is round trip ToA (RToA) also known as two way ToA ranging does not require precise synchronization [1, 33]. In ToA, ranging accuracy can be achieved with 2-3 cm error in LOS conditions [1, 6]. However, ToA estimation required a very wideband signal to estimate signal arrival time [49].

2.3.3. Time Difference Of Arrival (TDoA)

A slightly different version of ToA is called TDoA in which synchronization is required between participating ANs (i.e., minimum three ANs are required) rather than between TN and AN. In TDoA, TN is in listening mode and received signal time stamps (arrival time) from ANs. The time difference (TD) is estimated from propagation times, and these TDs create hyperbolas. From the hyperbolas, the position is estimated. The advantages of using TDoA are that more than one TNs can be localized simultaneously [33], and does not require AN-TN synchronization (good for mobile TNs). However, TDoA requires more calculations (processing) compared to ToA [49] and accuracy degraded under NLOS condition [50].

2.4. Wireless Standards Used for IL

2.4.1. Impulse Radio Ultra Wide Band (IR-UWB)

IR-UWB is the mode of short-range wireless communication in which very short pulses are transmitted with a minimum bandwidth of 500 MHz over a broad span of frequencies. It was first introduced by Guglielmo Marconi in 1901 to transmit Morse codes. However, with advancements

Chapter 2

and advantages of narrowband communication, it was abandoned. With the recent advancement in digital circuitry and digital signal processing, renewed interest have been developed towards (IR) UWB for its various advantages [6, 16, 51-53]. The prominent edge of IR-UWB is providing precision localization with an accuracy of 2-3 cm in LOS scenarios along with data communication [6, 54]. This advantage is inherent from transmitted pulses which have high resolution in time. For this reason, Federal Communications Commission regulated UWB and assigned operating frequency bands between 3.1 and 10.6 GHz with a cap on the emitting power of -41.6 dBm/MHz in band power spectrum density (PSD). The cap on power is due to the very large bandwidth of UWB which can interfere with other wireless systems. UWB is also standardized by various organizations such as Institute of Electrical and Electronic Engineering (IEEE) with standards 802.15.3a and 802.15.4a (IR-UWB). The detailed of IR-UWB can be found in [55, 56].

2.4.2. Wireless Local Area Network (WLAN)

WLAN is defined as a distributed wireless network of connected devices with an access point that can connect to the internet. WLAN operating frequency bands (such as 2.4 and 5.8 GHz) are a license-free spectrum. Due to this, it is the most commonly used wireless network worldwide. And is regulated through organizations such as IEEE (IEEE 802.11a/b/g/n). IL is enabled in WLAN with the help of RSSI ranging [31]. The distinct advantage of IL using WLAN is its low cost as WLAN deployments are commonly found.

2.4.3. Bluetooth

Bluetooth is developed for networking among personal and computer peripheral devices. The standard is designed for ease of wireless connectivity instead of using cables for short-range communication. Bluetooth is operated in 2.4 GHz frequency spectrum and is based on IEEE 802.15.3 standard [57]. Bluetooth standard is used in IL in which distance is estimated based on RSSI technique as in [43, 58].

2.4.4. Zigbee

Zigbee® standard is designed for applications which need low-power and low-bandwidth. The standard is based on IEEE 802.15.4 based specifications and globally operated at 2.4 GHz frequency [59]. Zigbee® is gaining popularity in home automation, medical device data collection,

Chapter 2

WSNs and in military applications because of its low-power and low-bandwidth operating characteristics [60, 61]. Zigbee based IL uses RSSI for ranging estimation [62, 63].

2.5. IL & IR-UWB

IR-UWB is an ideal candidate for IL in precision and accuracy demanding applications [16]. This is due to IR-UWB's prime advantage of providing high resolution positioning along with the following notable advantages [6, 55]:

- Adaptable data rates: suit well for both low-data-rate and high-data-rate applications.
- Low complexity hardware: As carrier-free transmission in which only very short radio frequency (RF) pulses are transmitted and received.
- High penetration capability: Due to very short pulses which have a high gain that can penetrate through the obstructions
- Very low power spectrum density (PSD) (-42 dBm/MHz): Due to this coexistence with another wireless system, and IR-UWB doesn't interfere with other wireless communication.
- Low energy consumption: due to PSD.
- Inherent Security feature: due to low power emission IR-UWB's communication appears to be below the noise floor for other wireless systems. And for these systems, IR-UWB's signals are treated as noise.

Due to the above-stated advantages, IR-UWB is adopted commercially and devices available from vendors such as Time Domain®, Decawave®, and Ubisense®. In this thesis, the IR-UWB standard is considered, and the accuracy and latency problem related to mitigating ranging error is considered in IR-UWB domain. In the following section, existing range error techniques with reference to the domain are discussed. First, positioning algorithms utilized in IR-UWB are discussed followed by ranging error techniques.

2.6. Positioning Algorithm Types

The mathematical models or calculations for estimating position that are implemented in computers or embedded systems are called position algorithms (PAs). Three types of PAs namely

Chapter 2

trilateration extended Kalman filter, and particle filter are discussed with reference to IR-UWB are as follows.

2.6.1. Least Square Trilateration

Trilateration is the geometric process in which the absolute or relative location of the point is estimated given distances using circles. For two dimensional (2D), three distances between ANs and TN are required. The distances are as follows:

$$d_i = \sqrt{(x_{TN} - x_{AN_i})(y_{TN} - y_{AN_i})}, \quad (2.1)$$

Where $i = 1, 2, \dots, n$ and $n \geq 3$, for 2D. . To establish our notations, let an TN be at an unknown position denoted by $P = (x_{TN}, y_{TN})$. The TN is surrounded by the number of ANs denoted by $N_a = n$ with known positions denoted by $A_i = (x_{AN_i}, y_{AN_i})$. In order to localize the TN, 2.1 need to be solved for unknown (x_{TN}, y_{TN}) . The coordinates are treated as the point of intersection of several spheres (or circles) whose center of location are A_i . The problem of estimating P falls under the least square (LS) domain. Furthermore, d_i is estimated using a ranging algorithm and denoted as \hat{d}_i . As 2.1 is nonlinear and the solution is also nonlinear LS and algorithm for finding P is given as:

$$\hat{P} = \arg \min_{TN} \sum_{(A_i, \hat{d}_i) \in O} (\hat{d}_i - d_i)^2, \quad (2.2)$$

where O are the number of agent-anchor pairs in the vicinity. For 2D, $\min O = 3$. The solution using (2.2) is not feasible because it produces a nonlinear equation of high degree [64]. So, the TN position can be estimated through minimizing (2.2) by solving numerically using pseudo inverse linearization method [64]. However, the solution does not consider ranging errors and \hat{d}_i should be close to d_i for accurate estimation of P .

2.6.2. Extended Kalman Filter (EKF)

Kalman filter (KF) is the type of recursive filter that falls under Bayesian Filters domain. KF estimate the current state of a system based on past estimations and current measurements. In the process, KF assumes that the system is linear with a Gaussian probability model. However, in tracking and navigation measurements (such as ranges, velocities, and accelerations) are nonlinear,

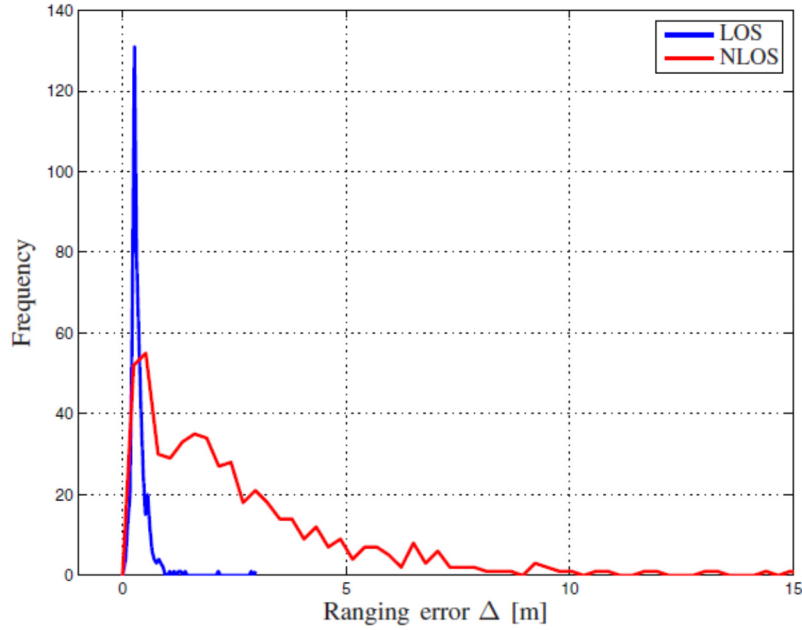


Fig. 2.2: Ranging error variation in LOS and NLOS conditions [3]

and KF performance degrades under these nonlinearities. So, KF is evolved into extended KF (EKF) or sigma point KF to address the nonlinearity problem. Also, in EKF, noise distributions are assumed to be Gaussian with proper tuning of covariance of the assumed probabilistic model. EKF is used in indoor tracking and navigation using it in IR-UWB is advantageous due to low computational complexity as in [65, 66]. However, the performance of EKF is highly depended on the proper tuning of covariance of the assumed probabilistic model and initial state estimation [2, 66].

2.6.3. Particle Filter (PF)

PFs are types of Bayesian filters which are applied to systems with nonlinear measurements and non-Gaussian distributions. In PF, the estimated TN's position is considered as samples rather than parametric density [67]. For this reason, PF can cope with nonlinearity and complex non-Gaussian distributions. PF is used in indoor tracking and navigation in general and particularly in IR-UWB domain as in [67, 68]. For instance, in [67], authors used PF for localization in underground mines for IR-UWB radar. The prime advantage of PF is its robust performance under nonlinearity and non-Gaussian distributed noise and disturbances. On the other hand, its prime disadvantage is its high computational complexity which overshadows its advantage in mobile devices [65].

2.7. NLOS Ranging error Mitigation Types

As a wireless technology, IR-UWB deployments experienced MPP and NLOS condition. Due to conditions persist in wireless systems, ranging errors are introduced to IR-UWB based IL systems.

Table 2.1: Existing studies for classification and mitigating NLOS ranging errors in IR-UWB

Method Based on		Parameters used	Position Algorithm	Classification/ error mitigation	Comments
Range statistics	[2]	Ranges std. deviation	BEKF	Classification, & Error mitigation	Bias are estimated for severity of NLOS
CIR parameters statistics	[5]		Weighted LS Trilateration	Classification & Error mitigation	Weights are derived for severity of NLOS
	[6]		NA	Classification	
Machine learning	[7]	Signal energy, max. amplitude, rise time, mean excess delay, RMS delay spread, Kurtosis	LS Trilateration	Classification, & Error mitigation	Regression is applied for error estimation
	[8]			Error mitigation	
	[9]			Classification	
CIR parameters	[10]	Received power, received first path power	LS Trilateration EKF	Classification & Error mitigation	Weights are derived for severity of NLOS
	[11]		EKF	Classification & Error mitigation	ToA estimations are corrected
Fuzzy logic based mapping	[12]	SNR, RMS delay spread, kurtosis, skewness		Classification & Error mitigation	Predefined errors are identified using fuzzy logic mechanism

Chapter 2

Therefore, in literature, techniques have proposed to mitigate these errors. The techniques that are available in the literature are summarized in Table 2.1, and a brief overview is presented as follow.

2.7.1. Range Statistics Based

This technique is based on multiple range measurements. With those measurements, the ranging errors' statistical parameters are estimated. The ranging error variations exhibit differently in LOS and NLOS conditions as illustrated in Fig. 2.1 [3]. Based on the variation, a weight can be assigned and accounted in biased EKF (BEKF) as studied in [2]. In [2], authors derived weights for mitigating NLOS ranging error from measured range statistics and modified measurement covariance of EKF which is called BEKF. The technique is simple and relies only on ranges. Therefore, it is also used in IL systems based on other standards such as in WLAN for mitigating the error [69, 70]. However, estimating online variance and standard deviation for moving TN is inaccurate particularly under NLOS conditions [65]. Moreover, latency is introduced due to multiple measurements' requirement which affects position updates. Also lost of information for using range statistics instead of CIR data [7].

2.7.2. CIR Data Based

In this technique, the range error bias is estimated using either CIR's statistical properties or CIR power profile property. In the case of a statistical solution, the properties for identification of LOS and NLOS and mitigation of ranging error due to NLOS are amplitude statistics and delay statistics. In [5], the authors investigate behavior of CIR's amplitude and delay statistics and derived weights proportional to the bias in NLOS condition based on the statistical characterization of the conditions. The weights are utilized in WLS to show position performance improvement under NLOS condition. The amplitude and delay statistical parameters' probability density function (PDF) are used namely kurtosis, mean excessive delay spread and root mean square (RMS) delay spread, for the identification and derivation of weights based on the severity of the NLOS condition. The proposed technique was evaluated based on simulated 802.15.4a (IEEE standard for IR-UWB) channel models. In [6], the authors used a similar method to [5] but using parameters such as kurtosis, skewness, peak-to-lead delay, power difference and power ratio. Moreover, the proposed work is assessed using real-time measurements in an industrial

Chapter 2

environment for the identification of LOS/NLOS. Similar to the range statistic based, CIR parametric statistic technique also introduced latency as because of statistically based solutions.

In case of power profile of CIR, received signal power and first path power at RX are used for identification of LOS and NLOS condition and weighting NLOS condition's severity. In [10], the author identified LOS, soft NLOS (i.e., direct path present) and severe NLOS (i.e., in which there are significant ranging errors) conditions based on power ratio. The power ratio is between received power and FP received power. After identifying severe NLOS, range correction and position estimation are based on geometric LS algorithm. In [11], authors implemented identification technique similar to [10] but corrected ToA estimation based on the empirically predefined standard deviation. ToA error variance for severe NLOS conditions. The corrected ToA estimation is used in EKF for estimating TN position.

2.7.3. Machine Learning Based

In this technique, the first step is to develop a model by training a machine learning mechanism such as least square support vector machine (LS-SVM). In a second step, the trained model is utilized to estimate range error bias and correct a ranging error using the bias. The model is trained using empirical CIR parameters as inputs and ranging errors as output. The parameters are the energy of the signal, rise time, max. signal amplitude, excess delay spread, and kurtosis. The technique is studied and proposed in [7, 9, 29]. In [7], authors suggested the LS-SVM model for the identification of LOS/NLOS and the mitigation of ranging error bias in NLOS condition. The proposed model training and its performance were evaluated using real-time experimental data. In [8], the authors suggested range errors bias mitigation in one step rather than two steps (i.e., identification and mitigation) procedure using LS-SVM technique. The authors stated the disadvantages of estimating ranging errors in two steps such as the crude way of dealing with ranging errors. In [9], the authors proposed a support vector data description (SVDD) machine learning methodology for ranging error mitigation which is also one step concept based. The study analyzed the percentage of training data and its impact on the ranging error mitigation accuracy. Although the above-stated machine learning based references identify NLOS conditions and mitigate range error bias due to NLOS condition, they are not feasible in the practical real-time system due to computational complexity [11]. Moreover, machine learning based methods are

Chapter 2

time-consuming due to mandatory training phase and highly dependable on the uncertainties of the environments.

2.7.4. Fuzzy Mapping Based Obstruction Identification

In [12], authors purposed obstruction identification based NLOS range error mitigation based on a fuzzy mapping between signal characteristics (inputs) and likely obstruction (output). The signal characteristics are signal-to-noise ratio (SNR), RMS delay spread, kurtosis and skewness for identification of predefined obstructions (propagations), namely, iron door, wood door, concrete wall, pedestrian, and corner. After identification, range error is compensated using predefined range error for a particular obstruction. The empirical designed fuzzy logic model is evaluated and validated in predefined propagations. However, CIR frame length data is required for estimating the signal characteristics. Moreover, acquiring CIR frame data in runtime adding a delay in estimating range between ANs and TNs [1].

2.8. Summary

In this chapter, the ranging definition, positioning metrics, different types of methodologies for ranging and different wireless standards used in IL are discussed. Also, it is showed that IR-UWB wireless standard provides better precision localization along with distinct features than other wireless standards. The overview of different positioning algorithms and their pros and cons with respect to usage in IR-UWB are presented. The literature review of existing range error mitigation and classification techniques using IR-UWB are also presented. The analysis of measured parameters collected in real time experiments is discussed in the next chapter. The analysis is the core for designing the rules on which classification and fuzzy logic are based.

3.1.Introduction

IR-UWB based devices are available commercially since the late 90s. However, these devices are streamlined after industrial standards (such as IEEE 802.15.4a) in earlier 2000s. Moreover, due to the advancement of digital and RF front end as well as potential applications of IR-UWB in different domains, proliferation, and availability of the devices are improved over the time. Due to this, recent research studies to address NLOS and MPP issues in IR-UWB are based on and validated using the devices [3, 6, 12]. In [3], design methodologies are empirically designed in different environments (i.e., office, universities, industries) using different scenarios by conducting and collecting data using experimental setups. So, it is vital to carry out empirical studies using an experimental testbed for a fair comparison with existing work. Moreover, the proposed solutions are more convincing and practical using experimental validation rather than simulation-based validation.

In this chapter, available devices, their features and comparison, and details of the selected device are presented first. Second, experimental setups in different environments, scenarios selection and placement of nodes are described. Third, parameters observations under different scenarios for LOS and NLOS conditions are analyzed. Finally, chapter conclusion is drawn in the summary section.

3.2.Device selection for experiments

3.2.1. Comparison of Decawave® & Time Domain® devices

There are many small and big manufactures of IR-UWB compliance devices. However, the prominent commercially available complete kits are from Decawave® and Time Domain®. Recently, Time Domain® are merged with Humatics® (www.humatics.com). The key characteristics of both the kits (i.e., from Decawave® and Time Domain®) are summarized in Table 3.1. From the Table, the main difference between EVK-1000 and PulseON® 410 is the sampling of the RF spectrum. Due to this Decawave® devices have a lower cost compared to Time Domain® devices at the cost of lower ranging accuracy. So, for the experimental studies, we chose Decawave® EVK-1000 kit.

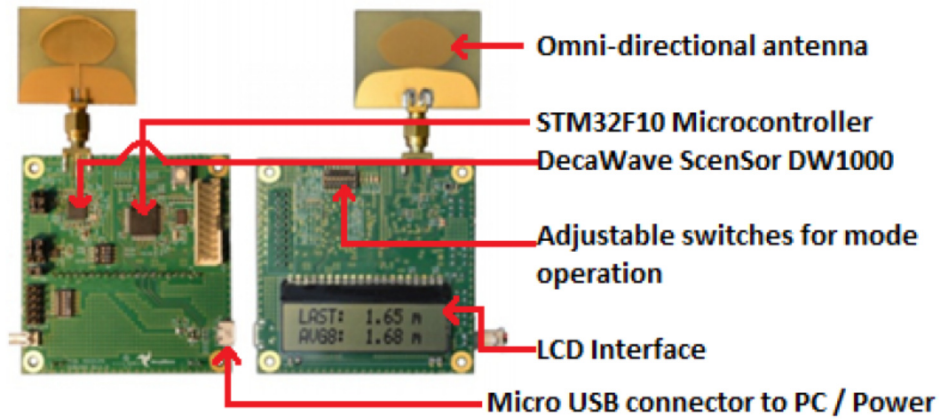


Fig. 3.1: EVK-1000 kit EVB-1000 nodes[1]

3.2.2. Decawave EVK-1000 Kit Description

- **Hardware**

The kit performs two-way ToA (TW-ToA) based ranging to estimate the distance between two nodes. It consists of two EVB-1000 boards (nodes) as shown in Fig. 3.1. Each board is equipped with DW-1000 chipset, ARM controller and omi-directional antenna. The heart of the board is DW-1000 radio CMOS chip which is fully integrated low power radio transceiver compliant with IEEE 802.15.4-2011 UWB standard. The chip consists of the analog front end (both RF and

Table 3.1: Key Characteristics of EVK-1000 & PulseON 410 kits

Characteristics	EVK-1000	PulseON [®] 410
Ranging Based on	TW-TOF	TW-TOF
Ranging Accuracy	Typically ± 3 cm (LOS Condition)	2 cm (LOS Condition)
Operating range	Upto 290 m @ 110 Kbps (LOS Condition)	Upto 500 m (LOS Condition)
Operating Frequency	3.5-6.5 GHz	FCC*: 3.1-5.3 GHz EU ETSI EN**: 3.1-4.8 GHz
Access technique	TDMA	ALOHA/TDMA
Average transmitted power	-41.3 dBm/MHz	-41.3 dBm/MHz
RF spectrum sampling rate	Sub Nyquist rate	Nyquist Rate (min.)
Regulation Compliance	FCC & EU ETSI EN	FCC & EU ETSI EN

*FCC: Federal Communications Commission

**EU ETSI EN: European Union European Telecommunications Standards Institute European Standard

Chapter 3

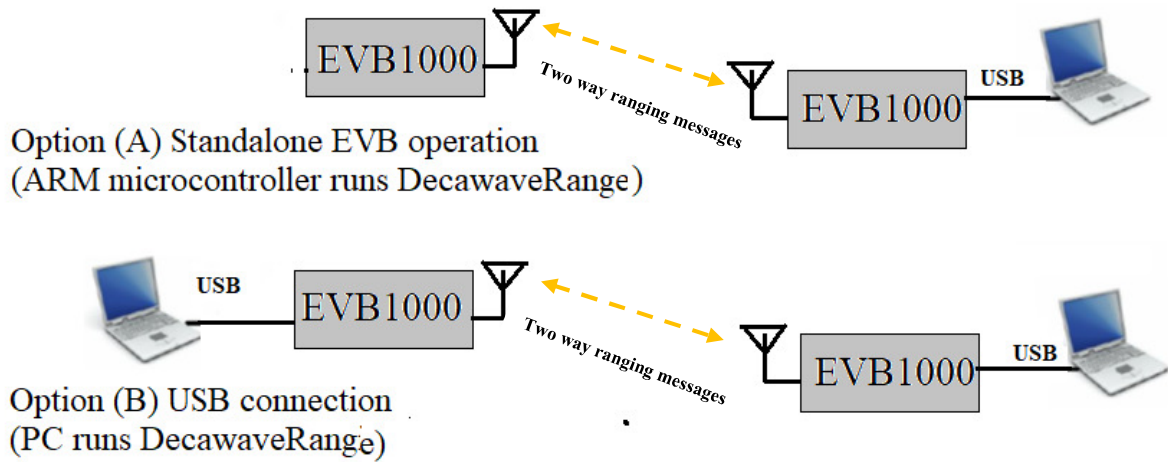


Fig. 3.2: Mode of Operation of EVK-1000 Standalone vs USB connection [1]

baseband) and a digital back-end interface to host processor (that control the chip). The chip's mode of operations are summarized in Table 3.2, and a detailed description along with data sheets can be found in [1]. The onboard USB or serial peripheral interface (SPI) ports support external application (or controller) to control the radio chip. Therefore, EVB-1000 board can be operated either in a standalone or USB connection or SPI connection modes as illustrated in Fig. 3.2. In the standalone mode, either one node or both nodes are operated on battery-powered and controlled by onboard ARM controller. The ranging information is displayed on the onboard LCD. In USB

Table 3.2: DW1000 Operating characteristics

Channel number	Centre frequency (MHz)	Bandwidth (MHz)	Preamble Codes (16 MHz PRF*)	Preamble Codes (64 MHz PRF*)
1	3494.4	499.2	1,2	9,10,11,12
2	3993.6	499.2	3,4	9,10,11,12
3	4492.8	499.2	5,6	9,10,11,12
4	3993.6	1331.2**	7,8	17,18,19,20
5	6489.6	499.2	3,4	9,10,11,12
7	6489.6	1081.6**	7,8	17,18,19,20
*Pulse Repetition frequency				
**DW1000 has a max. receive bandwidth of 900 MHz				

Chapter 3

(or SPI) connection, the ranging information is processed and manipulated in software that controls the radio chip.

- **Software**

Personal Computer (PC) based DecawaveRanging® software provides alternate to the onboard ARM-based embedded software which offers additional configuration, controlling, data logging, and diagnostic features. The software enables the following DW-1000 radio's capabilities to be observed, and tested:

- General operation of the transceiver IC on the supported channels and modes provided in Table 3.2 as it sends and receives data frames.
- LOS operations and range. The operational range can be checked by placing the receiver at various distances from the transmitter in LOS condition. This is tested in all supported channel modes as in Table 3.2.
- NLOS operations and range. The operational range can be checked when various obstructions are between the receiver and the transmitter giving an NLOS channel. This is tested in all supported channels modes as in Table 3.2.
- Time-of-Flight (TOF) Ranging Measurements: The software performs 2-way ranging between the two nodes, and estimates the distance between them based on the TOF calculations. The operation is checked in LOS and NLOS and effects are observed on the distance estimation under LOS and NLOS as the two nodes are moved nearer/further from each other, and when there are walls and other obstructions between the units. Moreover, the nodes are tested in all supported channel modes mentioned in Table 3.1 for three different supported data rates (i.e., 0.11, 0.85 and 8.5 Mbps). In the observations, the distances are recorded along with the following data:
 - Logging of CIR data under LOS and NLOS.
 - Logging of SPI activities.

It was found that there is no significant impact of different channel modes for LOS and NLOS operations and ranging estimation under the conditions.

Chapter 3

3.3. Scenarios for experimental setups

We collected measurements in two different environments, (i.e., Office and Warehouse). The locations of selected areas are inside the engineering building of the University of Windsor. In both environments, the nodes are placed on trapezoids to collect measurements as shown in Fig. 3.3 & 3.4. The LOS and NLOS scenarios are created by placing TX and RX nodes at different intervals between 1.92 m and 11.31 m. The NLOS scenarios are emulated using the signal wall, multiple walls, concrete, and metal pillars, glass wall, the human body and different objects (i.e., chairs, metallic parts, etc.). The NLOS obstructions in each scenario are summarized in Table 3.3. In all, there are 30 scenarios where 700 measurements of the parameters are collected. The characteristics of the two locations are different which are as follows.

3.3.1. Office Scenario

Table 3.3: Scenarios (and their abbreviations) and Obstructions

Scenario	Abbreviation	Obstruction
Office 1 wall	O1W	One wall
Office 2 wall	O2W	Two wall
Office 3 wall	O3W	Three wall
Office Multi-wall	O4MW1	Multi wall
Office Multi-wall	O5MW2	Multi wall
Office Glass	OG1	Glass (clear)
Office Glass	OG2	Glass (Opaque)
Warehouse 1	W1B1	Box
	W1M1	Metal
	W1M2	Metal (nodes @height 4 ft. from ground)
Warehouse 2	W2H1	Human
	W2M1	Metal
	W2M2	Metal (nodes @height 4 ft. from ground)
Warehouse 3	W3M1	Metal
	W3T1	Trolley
Warehouse 4	W4M1	Metal
	W4M2	Metal (nodes @height 4 ft. from ground)
	W4T1	Trolley
	W4T2	Trolley (nodes @height 3 ft. from ground)
Warehouse pillar	WP1	Metal Beam (Pillar) to support roof

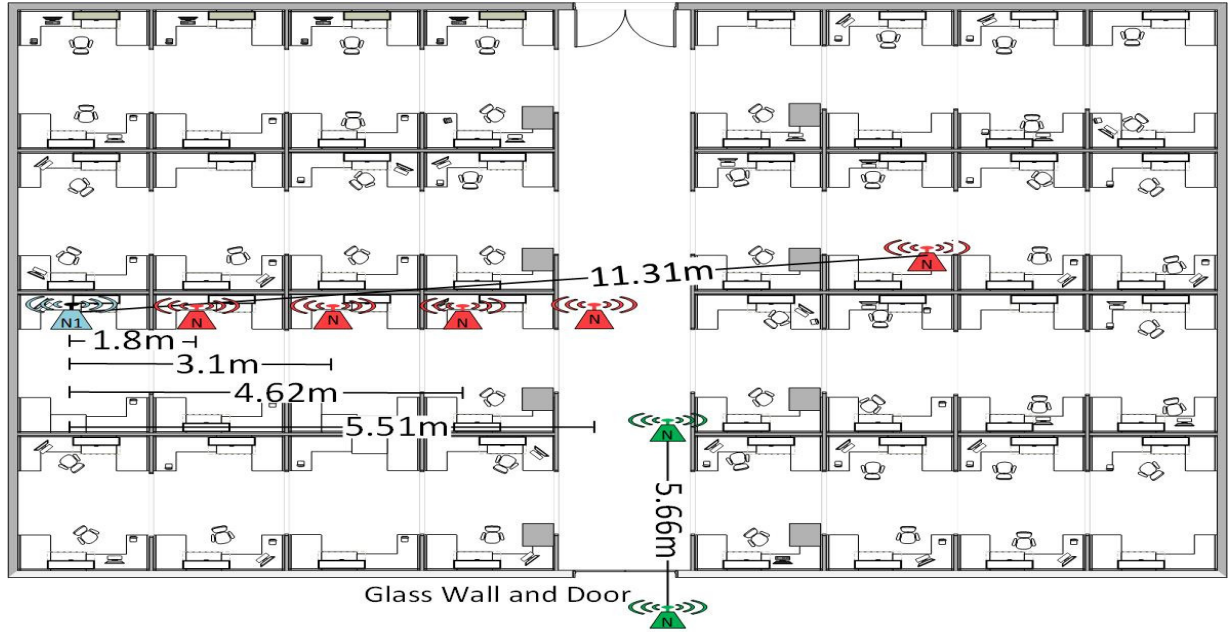


Fig. 3.3: Office Floor plan

Office setup has cubical spaces separated by wooden separators of 5 feet height. The office area is 30x20 meters square (m²). In the office, cubical spaces are created using wooden wall separation and concrete pillars. In each cubical space, desk, chair, and metal cabinet are placed. There are also glass walls that enclosed the area. The detail of nodes placement along with office floor plan are illustrated in Fig. 3.3.

3.3.2. Warehouse Scenario

The dimension of the warehouse is 20x50 m². In the warehouse, the area is designated as research and development for automobile engines and parts. It has metal pillars. The area is kind of open space with metal parts that mimic an industrial environment. The detail of nodes placement along with warehouse floor plan are illustrated in Fig. 3.4.

3.4. Observations of different parameters in scenarios

3.4.1. Received Signal Strength (RSS)

Instantaneous (Inst.) RSS is estimated in Decawave devices using [1]:

$$RSS (dBm) = 10 \log_{10} \left(\frac{{}^C(K)}{N^2} \right) - A \quad (3.1)$$

Chapter 3

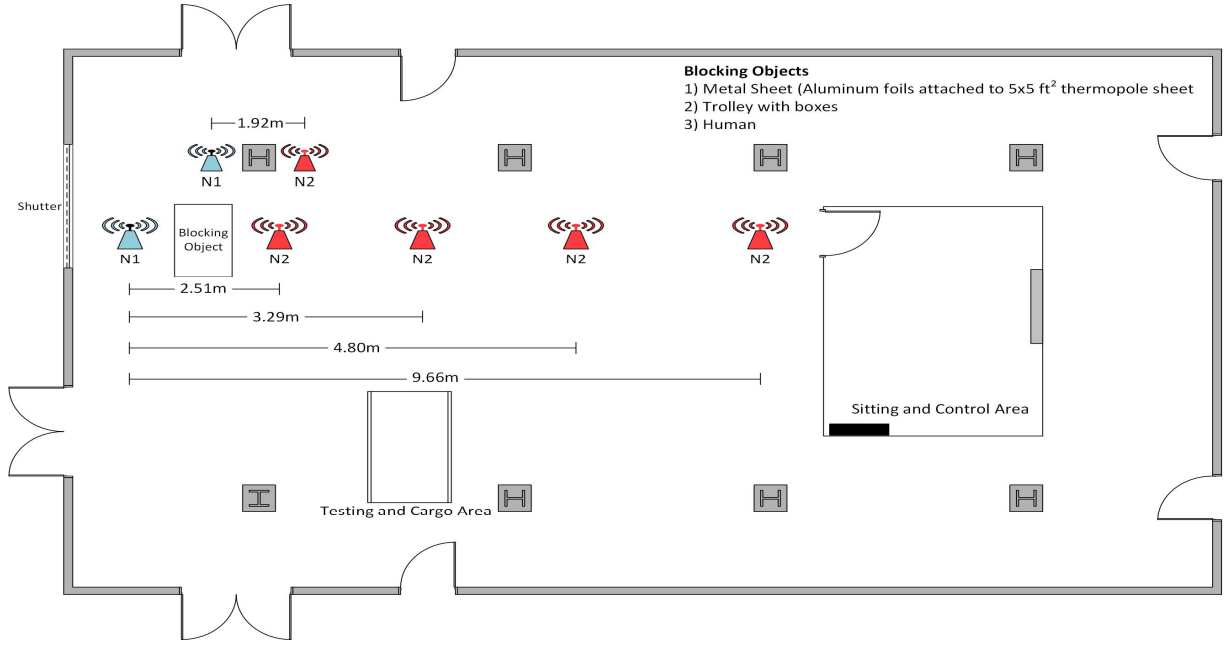


Fig 3.4: Warehouse Floor Plan

where C is the CIR magnitude, N is the preamble accumulation count, K is constant of 2^{17} , and A is a predefined constant of -115.72 dBm for a Pulse Repetition Frequency (PRF) of 16 MHz or -121.74 dBm for a PRF of 64 MHz. Probability density functions (PDFs) of RSS in LOS, soft NLOS (SNLOS) (i.e., in SNLOS direct path is the strongest path) and NLOS conditions are illustrated in Fig. 3.4(a). From the figure, it can be inferred that in LOS and SNLOS the RSS values are centered around -80 dBm. However, in the case of NLOS, RSS value is concentrated around -83 dBm. From the PDFs, it is obvious that RSS is decreased in NLOS conditions due to obstructions. As more severe the NLOS condition is the more power is lost due to the nature of obstruction and number of obstructions. Moreover, LOS and NLOS conditions can be identified based on RSS values as shown in Fig. 3.4 (a). However, in some cases where RSS decreased to -84 dBm in the case of SNLOS and LOS. Also in NLOS case, it increased to -80 dBm. The area is identified as a grey area, and the region is where misclassification occur for only based on inst. RSS value.

3.4.2. First Path Signal Strength (FPSS)

Inst. FPSS is estimated using F_1 and two more CIR's components (i.e., F_2 and F_3) followed by F_1 as [1]:

Chapter 3

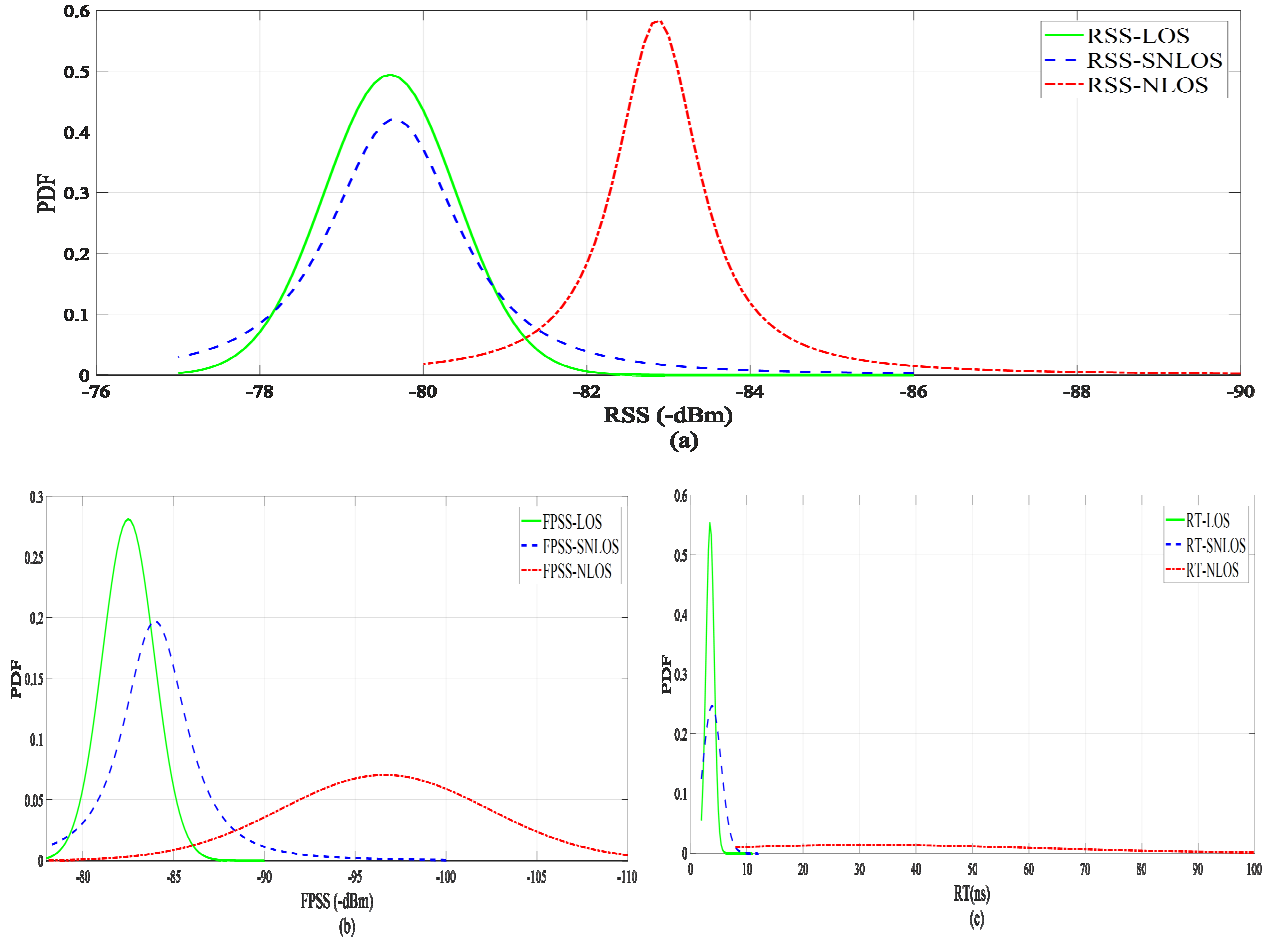


Fig. 3.5: Parameters PDF in different scenarios: (a) RSS; (b) FPSS; (c) RT

$$FPSS \text{ (dBm)} = 10\log_{10} \frac{(F_1^2 + F_2^2 + F_3^2)}{N^2} - A, \quad (3.2)$$

From 3.1 and 3.2, inst. RSS and FPSS are correlated to each other as both are estimated using CIR values. So, FPSS exhibit similar to RSS in LOS, SNLOS, and NLOS as illustrated in Fig. 3.5(b). However, FPSS is also attenuated depend on first path attenuation factor (more detailed analysis and the relationship between RSS and FPSS will be discussed in Chapter 5).

3.4.3. Rise time (RT)

RT is defined as the difference between the time occurrence of the strongest path in $h(t)$ (F_s), denoted as T_{F_s} and time occurrence of leading edge (F_1), denoted as T_{F_1} as given:

$$RT(nsec) = T_{F_s} - T_{F_1}, \quad (3.3)$$

Chapter 3

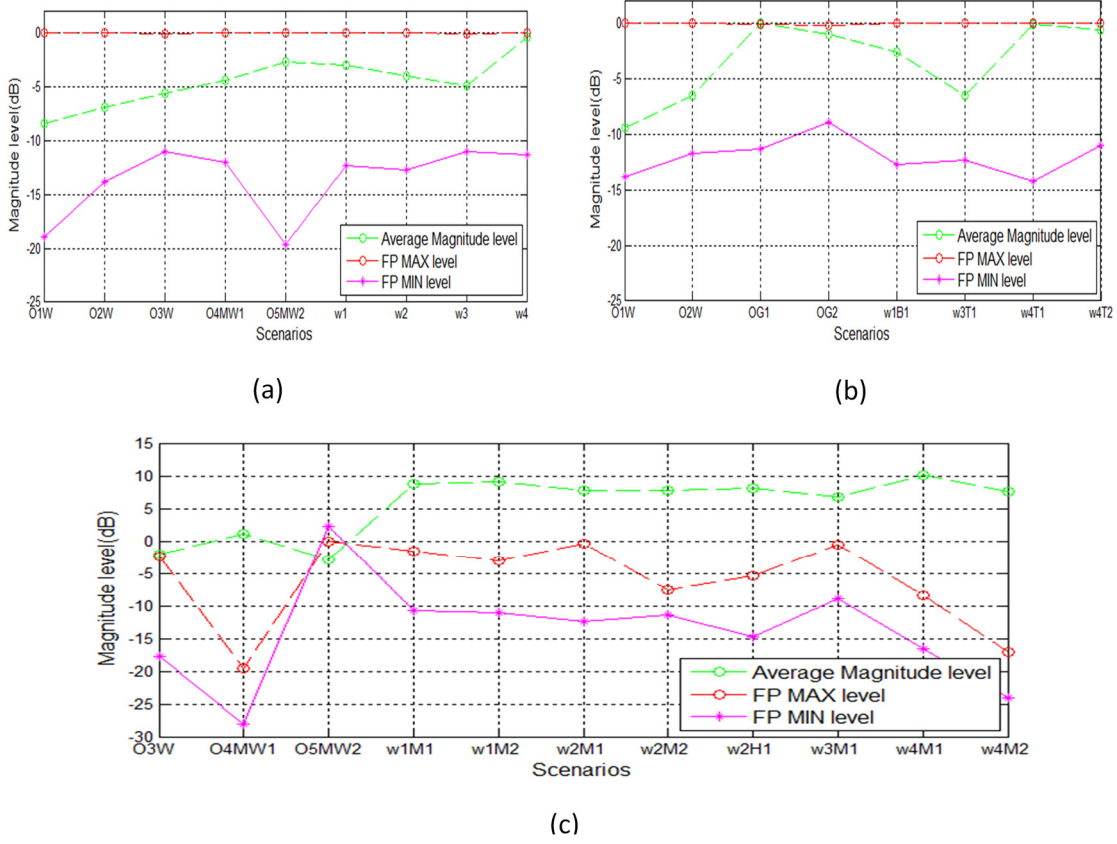


Fig. 3.6: Average magnitude (M_{AVG}), FP-Min (M_{LEP}), and FP-Max (M_{FPM}) levels in different scenarios

RT's PDFs for LOS, SNLOS, and NLOS are given in Fig. 3.5 (c). From empirical PDF observation, it is obvious that strongest path is the first path in LOS and SNLOS cases as RT's PDFs are concentrated on the lower side (i.e., between 2 to 6 ns) as illustrated in Fig. 3.5 (c). Whereas, in NLOS case, values are much higher (greater than 10 ns) because the strongest path in NLOS is not the first path.

3.4.4. Average CIR normalized magnitude

It is estimated using CIR $h(t)$ normalized magnitudes as given:

$$M_{AVG} = 10 \log \left[\frac{\sum_{i=t_{LEP}}^W \log[h(t_i)]}{W - t_{LEP}} \right], \quad (4.1)$$

where t_{LEP} is the leading edge time at which the range is estimated based on Time of Arrival (ToA) technique, and W is the frame size in a nanosecond (ns) where discrete $h(t)$ presents. In the case of Decawave devices, W is 1016 ns [1].

Chapter 3

3.4.5. Leading Edge Normalized Magnitude

It is estimated using the first normalized magnitude above threshold (δ) occurs in $h(t)$ at the time denoted as t_{LEP} (i.e., $h(t_{LEP})$). It is also called the first path (FP) minimum and its magnitude is computed as:

$$M_{LEP} = 10 \log[h(t_{LEP})], \quad (4.2)$$

3.4.6. First Path Max Normalized Magnitude

It occurs in $h(t)$ either at the time: $\alpha_1 = t_{LEP} + 1(\text{ns})$ or at the time: $\alpha_2 = t_{LEP} + 2(\text{ns})$, depends on which CIR's magnitude level is higher (i.e., $\max|h(t_{\alpha_1}), h(t_{\alpha_2})|$). It is estimated as:

$$M_{FPM} = 10 \log[h(t_{\alpha_i})], \quad (4.3)$$

where $i \in \{1 \text{ or } 2\}$.

The parameters' (i.e., M_{AVG} , M_{LEP} , and M_{FPM}) average values in different scenarios are illustrated in Fig. 3.6. From the figure, M_{AVG} has lower values in LOS and SNLOS compared to NLOS conditions. This is due to the strongest path in CIR's $h(t)$ in LOS and SNLOS and all other multipath components (MPCs') magnitudes in $h(t)$ are weak. Whereas in NLOS, the direct path (i.e., between TX and RX) is relatively weak and others MPCs are strong due to reflected, defracted and shadowed paths and direct path is partially or fully blocked by the obstruction. Due to this reason, M_{FPM} has the strongest magnitude in LOS and SNLOS conditions and lower magnitudes compared to other MPCs in NLOS conditions.

The parameters' observations are helpful in identifying the conditions (i.e., LOS and NLOS) and induced errors due to these conditions. The identification and mitigating the errors are covered in the next two chapters.

Chapter 3

3.5. Summary

In this chapter, first, availability of devices from leading vendors, their differences and selected devices description is presented. Also, the need for empirical based studies for designing and validating of the proposed methodology is emphasized. Second, scenarios creation in the selected premises is described. Third, measured parameters in the scenarios and their observations in different scenarios are presented.

A PARAMETRIC RULE-BASED CLASSIFICATION AND LOCALIZATION ALGORITHM FOR IR-UWB

4.1. Introduction

Wireless Sensor Networks (WSNs) are deployed in indoor and dense environments where Global Positioning System (GPS) does not perform satisfactorily [14]. Therefore, indoor Real-Time Localization System (RTLS) is an optimum choice to support applications demanding location awareness in the WSN domain [21, 22]. There are many existing wireless systems that support indoor localization along with data communication. The most popular of these systems are WiFi, Zigbee, Bluetooth and IR-UWB [16, 42, 71]. Among them, IR-UWB is at the forefront of providing high-resolution localization [11]. Besides precision ranging, IR-UWB salient features such as through-wall propagation, low power consumption, size form factor, and many other salient features bode well for WSN [16, 55]. However, the localization accuracy of IR-UWB degrades when they operate under NLOS conditions which are inherent in wireless communications with real-time deployments [5, 40]. Due to NLOS conditions, ranging errors increase significantly compared with LOS conditions.

Therefore a novel rule-based technique for classification of LOS and NLOS conditions along with geometric ranging correction methodology is proposed to minimize position errors under NLOS condition. The classification technique is designed with consideration of key requirements of WSN such as reduced computational requirement, delay due to measurements acquisition while enhancing classification accuracy for detecting LOS and NLOS conditions. The set of rules, on which classification is based, consider six specific parameters namely (I) average of normalized channel impulse response (CIR) magnitudes, (II) first path minimum CIR magnitude, (III) first path maximum CIR magnitude, (IV) received signal strength, (V) first path signal strength and (VI) rise time. For range mitigation, a geometrical ranging correction positioning algorithm based on the geometrical layout of anchors and agent nodes is proposed. Moreover, experiments in two different scenarios are conducted to collect ranging data, signal levels and channel data in LOS and NLOS conditions. The experimental study and parametric data from Chapter 3 are used to support the proposed classification and range mitigation algorithm. Similar to [72], the proposed

Chapter 4

range mitigation algorithm is developed based on the assumption of having only one anchor-agent in NLOS condition. Furthermore, a probabilistic model is also presented to show simultaneously one anchor node out of three is the most likely in NLOS condition. The model justifies that the assumption of one anchor in NLOS in the ranging algorithm. The proposed classification and mitigation algorithm has low complexity and computational requirements while enhancing the position accuracy under NLOS condition without adding the delay in range acquisition.

The chapter is organized as follows: Section 4.2, discusses the classification of LOS and NLOS. Section 4.3, describes the probabilistic model, and a ranging algorithm. Experimental measurements and scenarios are presented in Section 4.4. Section 4.5, introduces the proposed algorithm and its performance and finally, the conclusions are provided in Section 4.6.

4.2. Classification of LOS and NLOS

4.2.1. Salient features in LOS and NLOS

From the preceding chapter explained that normalized MPCs are stronger in NLOS compared to LOS. Also, the strongest MPC is observed followed by leading edge of MPC in the first path in LOS condition. In addition to leading edge, two more MPC components constitute the first path (or the direct path) [1]. However, in NLOS condition the phenomena do not exhibit. Moreover, overall received power and first path power are attenuated in NLOS due to obstructions between the TX and RX and multipath propagation of the transmitted signal. Based on the parameters and channel magnitudes observations in the preceding chapter, following parameters are supportive in the identification of LOS and NLOS: Average CIR normalized magnitude, leading edge

TABLE 4.1: PARAMETERS OBSERVATIONS IN LOS AND NLOS

S. No.	Observation	LOS	NLOS
P1	M_{FPM}	$M_{FPM} = 1$	$M_{FPM} < 1$
P2	Relationship between M_{FPM} and M_{AVG}	$\mu M_{AVG} \leq M_{FPM}$	$\mu M_{AVG} > M_{FPM}$
P3	Relationship between M_{FPM} and M_{LEP}	$\beta M_{LEP} \leq M_{FPM}$	$\beta M_{LEP} > M_{FPM}$
P4	Relationship between M_{AVG} and M_{LEP}	$M_{LEP} \leq M_{AVG}$	$M_{LEP} > M_{AVG}$
P5	RT	$RT \leq 6$ ns	$RT > 6$ ns
P6	RSS	$RSS \geq -82.5$ dBm	$RSS < -82.5$ dBm
P7	Relationship between RSS and $FPSS$ (Δ)	$\Delta \leq 7$ dB	$\Delta > 7$ dB

Chapter 4

magnitude, the first path max magnitude, rise time, received signal strength (RSS), and the received first path's power.

4.2.2. Classification Methodology

Through extensive experiments in different scenarios in two different conditions (i.e., LOS and NLOS), observations regarding parameters are summarised in Table 4.1. The multiplier constants (i.e., μ and β) values are found experimentally which are 8 and 10 respectively. In addition to the observations, combining two or more observations for identifying the conditions is more effective and reduce false alarms (for classification) rather than using sole observation for identification. The observations' combination is called rules, and the particular combination is based on the following facts:

- Combination-1: P2 & P3
 - The combination is based on observations 2 & 3 (i.e., P2 & P3) from Table 4.1
 - Average magnitude of CIR (tells the no. of Multipath)
 - First path max. magnitude (tells the strength of the first path in LOS or NLOS)
 - First path min. magnitude (critical for range estimation in ToA algorithm)
 - Combination is based on CIR magnitudes
- Combination-2: P4 & P5
 - The combination is based on observations 4 & 5 (i.e., P4 & P5) from Table 4.1

TABLE 4.2: IDENTIFICATION RULES FOR LOS/NLOS

Identification	Rule# 1 (R1)	Rule# 2 (R2)	Rule # 3 (R3)	Combination	Logical Operation	Rule Logic
LOS	$\mu M_{AVG} \leq M_{FPM}$	$\beta M_{LEP} \leq M_{FPM}$		1	R1&R2	TRUE(1)
LOS	$M_{LEP} \leq M_{AVG}$	$RT \leq 6$		2	R1&R2	TRUE(1)
LOS	$\beta M_{LEP} \leq M_{FPM}$	$RSS \geq -82.5$		3	R1&R2	TRUE(1)
LOS	$RT \leq 6$	$RSS \geq -82.5$	$\Delta \leq 7$	4	R1&R2&R3	TRUE(1)
NLOS	$\mu M_{AVG} > M_{FPM}$	$\beta M_{LEP} \leq M_{FPM}$		1	R1&R2	FALSE(0)
NLOS	$M_{LEP} > M_{AVG}$	$RT > 6$		2	R1&R2	FALSE(0)
NLOS	$\beta M_{LEP} > M_{FPM}$	$RSS < -84.5$		3	R1&R2	FALSE(0)
NLOS	$RT > 6$	$RSS < -84.5$	$\Delta > 7$	4	R1&R2&R3	FALSE(0)

Chapter 4

- Average Magnitude
- First path min. magnitude
- Rise time (tell where in time span max. path occurs in CIR)
- Combination-3: P3 & P6
 - The combination is based on observations 3 & 6 (i.e., P3 & P6) from Table 4.1
 - Average magnitude
 - First path min. magnitude
 - Received power strength (tells how strong overall signal is)
- Combination-4: P5, P6 & P7
 - The combination is based on observations 5, 6 & 7 (i.e., P5, P6 & P7) from Table 4.1
 - Based on the received signal and the first path. The relationship holds well in mild NLOS conditions
 - Received signal strength exhibit differently in sever NLOS conditions
 - Does not require whole CIR data within the frame (i.e., 1016 data samples)

The above combinations are logically combined using AND operation for classification. Due to the fact that all parameters within particular combination are within a specific threshold (which are defined in Table 4.1) for LOS and logically true for LOS condition; that's why AND operation is appropriate. Truth Table for all the combinations along with the classification of LOS and NLOS are summarized in Table 4.2.

4.3. Range Mitigation Methodology

After classification, geometric range correction of one anchor-agent pair out of three is presented. First, one out of three anchor-agent pair's channel condition is in NLOS most probable occurrence analysis is presented. Second, the range correction of the pair method is presented.

In a typical non-industrial environment, anchors are located near ceiling level. Thus, most obstructions are generally avoided due to anchors elevation. In this case, it has been observed, during the experiments performed in real time indoor deployments that AN in LOS is most likely rather than in NLOS. So, having AN in LOS is assume to be $P_{LOS} = 70\%$ and that of NLOS is $P_{NLOS} = 30\%$ instead of equal probability. Based on the assumption, the probability of an AN experiencing NLOS, $P_{NLOS}(A_i)$ out of three ANs is modelled as:

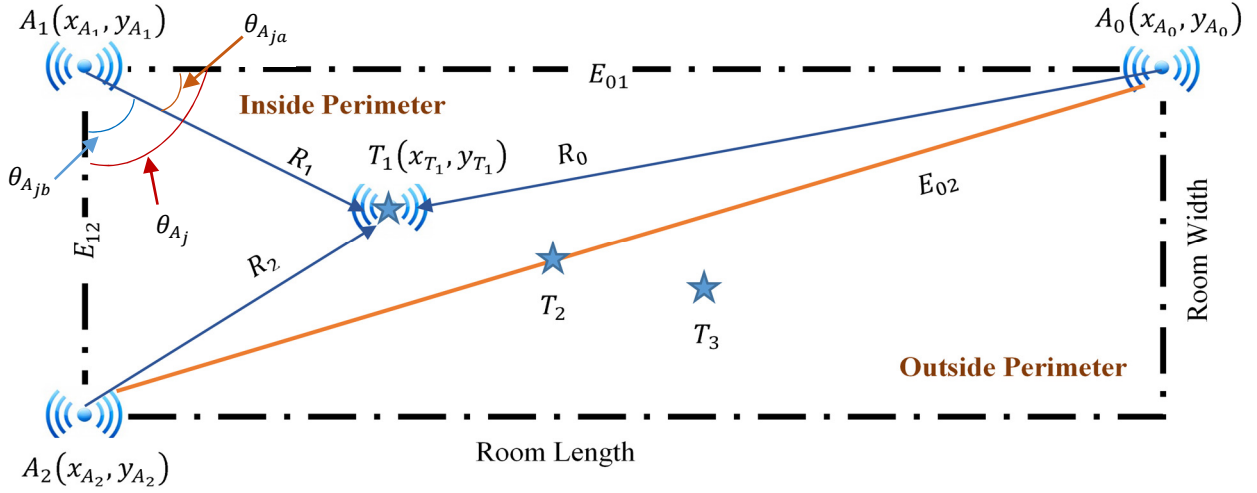


Fig. 4.1: Anchors and agent nodes placement

NLOS Probability for one anchor:

$$P_{NLOS}(A_i) = \binom{3}{1} P_{LOS} (1 - P_{LOS})^2, \quad (4.1)$$

where $i \in \{0,1,2\}$, and $P_{NLOS}(A_0), P_{NLOS}(A_1) \dots P_{NLOS}(A_N)$ are statistically independent events that shows either A_0 or A_1 or $\dots A_N$ is in NLOS respectively. The probability for two ANs experiencing NLOS simultaneously is as follows:

$$P_{NLOS}(2A_i) = \binom{3}{2} P_{LOS}^2 (1 - P_{LOS}) \quad (4.2)$$

From (4.1) and (4.2), it can be deduced that most likely single node experienced NLOS and co-occurrence of two or three anchor nodes in NLOS are less probable. Therefore, a single node experiencing NLOS should be handled with the highest priority, while there is a possibility of two or more anchors being NLOS, it is assumed in the range mitigated model that anchors are placed near ceiling level and that they are placed in strategic locations to minimize NLOS probability of two or three anchor nodes simultaneously. Based on the analysis, geometric range correction of any one of the anchor-agent pair out of three are as follows:

The distances between anchors, associated angles, and two LOS estimated ranges are required for geometrically correcting NLOS range as illustrated in Fig. 4.1. The distances between anchor

Chapter 4

nodes for known anchors' position and angles θ_{A_0} , θ_{A_1} , and θ_{A_2} associated with anchors A_0 , A_1 and A_2 are calculated respectively as follows:

$$E_{jk} = \sqrt{(x_{A_j} - x_{A_k})^2 + (y_{A_j} - y_{A_k})^2} \quad (4.3)$$

$$\theta_{A_j} = \cos^{-1} \left\{ \frac{E_{kl}^2 - (E_{lj}^2 + E_{jk}^2)}{(-2)E_{kl}E_{jk}} \right\} \quad (4.4)$$

where $(j, k, l) \in \{0, 1, 2\}$, $j \neq k \neq l$. Using the distances between anchors (i.e., from (4.3)), associated angles (i.e., from (4.4)) and two LOS ranges (R_j and R_k), the third range R_l can be corrected given A_l -agent pair is in NLOS using:

$$\theta_{A_{ja}} = \cos^{-1} \left\{ \frac{R_k^2 - (E_{jk}^2 + R_j^2)}{(-2)E_{jk}R_l} \right\} \quad (4.5)$$

$$\theta_{A_{jb}} = \theta_{A_j} - \theta_{A_{ja}} \quad (4.6)$$

$$R_l = \sqrt{E_{lj}^2 + R_j^2 - (2E_{lj}R_j \cos(\theta_{A_{jb}}))} \quad (4.7)$$

- For Point outside $\Delta A_0 A_1 A_2$:

For tag outside the triangle, the R_1 and associated angle ($\theta_{A_{0b}}$ or $\theta_{A_{2b}}$) for estimating R_1 are changed. However, R_0 or R_2 would not change due to geometric symmetry and can be corrected using (4.5, 4.6, and 4.7). For determining R_1 , the associated angle can be calculated by modifying (4.6) as :

$$\theta_{A_{jb}} = \theta_{A_j} + \theta_{A_{ja}} \quad (4.8)$$

where in this case $j \in \{0 \text{ or } 2\}$. For range R_1 to be determined outside the perimeter of $\Delta A_0 A_1 A_2$, it is required that to check whether the agent with position T is inside or outside the triangle $A_0 A_1 A_2$ as illustrated in Fig. 4.1. It can be checked as:

$$\gamma = \frac{\det(TA_2) - \det(A_0 A_2)}{\det(A_1 A_2)} \quad (4.9)$$

$$\vartheta = -\frac{\det(TA_1) - \det(A_0 A_1)}{\det(A_1 A_2)} \quad (4.10)$$

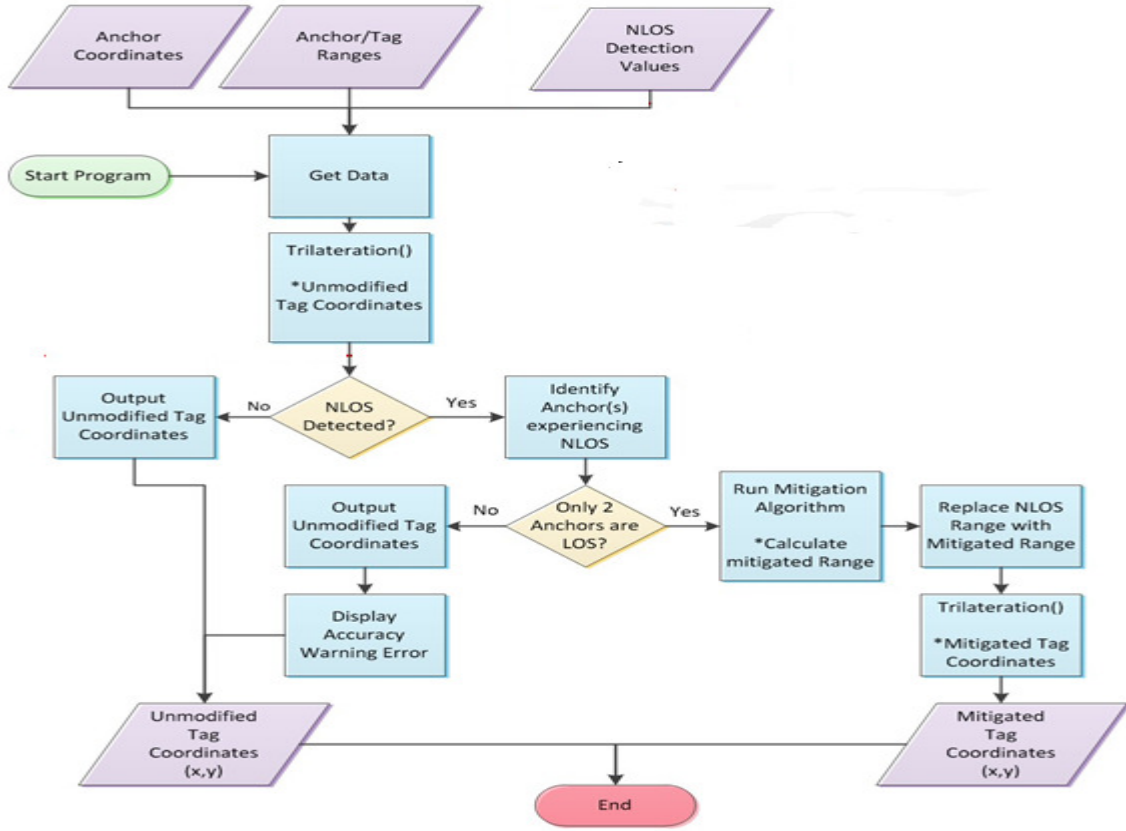


Fig. 4.2: Flow-chart of the proposed algorithm

$$\det(u \ v) = u \times v = u_x v_y - u_y v_x \quad (4.11)$$

For the point T_i (where $i \in \{1,2,3\}$) is inside $\Delta A_0 A_1 A_2$ if $\gamma, \vartheta > 0$ and $\gamma + \vartheta < 1$ otherwise outside the triangle. The flow chart of the proposed classifier and range mitigation algorithm is given by Fig. 4.2. From the figure, the algorithm starts with getting range values, ANs' coordinates, and condition (i.e., LOS or NLOS) identification from three ANs. In the second step, trilateration process is executed for estimating the position. If LOS for all ANs is present, then the estimated position is available at the output. If NLOS is detected, then the algorithm is checked for the number of ANs in NLOS. If one AN in NLOS is detected, then the range mitigation is applied to the NLOS range, and position is estimated with the corrected range. Otherwise, the unmitigated position is available with a range error warning at the output.

Chapter 4

4.4. Experimental Data

For validating proposed classification and ranging methodology, data collected in two different scenarios (i.e., Office and Warehouse) is used as described in Chapter 3. The data is comprised of ranges (i.e., R_0 , R_1 , and R_2) and associated CIR measurements. The data is collected in LOS and NLOS conditions at three different locations (i.e., T_1 , T_2 , and T_3) in each scenario. Three different locations in each scenario are depicted in Fig. 4.1. From CIR measurements, the parameters describe in Section 3.4 are extracted. In each of the scenarios, 400 set of ranges and CIR measurements were taken for LOS and NLOS conditions. So, in all 1200 measurements were taken in all scenarios.

4.5. Results & Discussion

In this section, the performance of the proposed classifier, range mitigation, and localization algorithm using a mitigated range are demonstrated. The performance measures and quantitative details are discussed.

4.5.1. Classification Performance

Performance of the classification strategies from Table 4.2 is quantified in terms of the confusion matrix as given in Table 4.3. The matrix is defined in terms of true positive (TP), true negative (TNa), false positive (FP) and false negative (FN). In addition, the terminologies are defined as:

- TP: LOS predicted when there is LOS condition present.
- TNa: NLOS predicted when there is NLOS condition present.
- FP: LOS predicted when there is NLOS condition present.
- FN: NLOS predicted when there is LOS condition present.

Misclassification rate (P_T) is defined in terms of false positive rate (FPR), and false negative rate (FNR) [7] as given:

$$P_T = (FPR + FNR)/2, \quad (4.12)$$

where $FPR = FP/N$ and $FNR = FN/N$. Where N is a total number of measurements (i.e., 1200). From Table 4.3, it is observed that FP and FN are the highest for Combination-2. FN is highest for the combination is due to less the MPCs in some LOS conditions and M_{AVG} is low in the conditions. Comparing with M_{LEP} , the statement (i.e., $M_{LEP} \leq M_{AVG}$) is false and detected as NLOS rather

Chapter 4

than LOS. Same is true for FP in conditions where there is severe NLOS present. In the LOS condition, most of the MPCs are relatively weak compared to first path MPC (strongest MPC) and these MPCs are below a threshold level in the threshold based detector. As there is no weightage for the MPCs below the threshold in the computation of M_{AVG} therefore M_{AVG} is low. For Combination-4, FN is the second highest in the Table. This is due to $\Delta > 7$ dB in some experimental setups where there are significant MPCs and the first path is detected earlier than the actual first path. Due to this, the first path power is low and the difference between the received signal and the first path is more than 7 dB. However, Combination-4 is most effective among different combinations for detecting NLOS conditions as depicted in the Table. Moreover, the combination requires only the parameters which are readily estimated in Decawave deceives [1]. It also does not introduce a delay due to non-requirement of CIR data from the devices [1]. Due to these facts, Combination-4 is considered from thereon.

To show the effectiveness of the proposed classifier, we compare the proposed classifier with presented in [40] and [7] as shown in Fig. 4.3. For classifier in [40], the solution is based on the difference between received signal and first path signal strengths and for LS-SVM classifier from [7], the best classification is based on the cumulative energy of the signal, the kurtosis of the

Table 4.3: Confusion Matrix

Rule Type	Number of measurements N=1200	Predicted LOS	Predicted NLOS
Combination-1	Actual LOS	465	35
Combination-2		401	99
Combination-3		493	7
Combination-4		460	40
Combination-1	Actual NLOS	36	664
Combination-2		44	656
Combination-3		30	670
Combination-4		4	696

Chapter 4

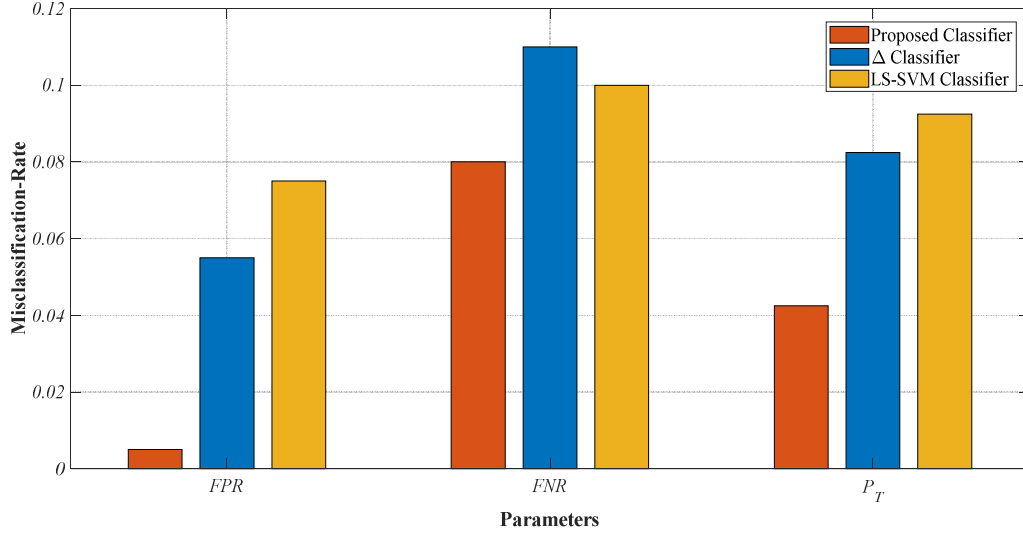


Fig. 4.3: Performance comparison of different Classifiers.

channel and rise time parameters. For a fair comparison, we extracted the parameters from our measurement database for both comparisons.

It has been observed that the proposed classifier is very effective in detecting NLOS condition for severe NLOS situations where the signal strengths are attenuated significantly (i.e., less than -85dBm) for the received, and the first path signals strength. However, due to less difference in the received signal and the first path signal strengths, the classifier in [40] failed to identify the condition and falsely detect condition as LOS. In the NLOS condition, ranging error is observed around 1 m. Due to attenuation, most MPCs preceding strongest path in CIR are below the threshold level, and the MPC closest to strongest MPC is detected as leading edge, so the difference between the first path signal strength (strongest path) and the received signal strength is less than 6 dB. Due to this, only difference based solution failed from [40] in the condition. In the case of LS-SVM classifier [7], the outlier increased in NLOS conditions due to the varying condition of the channels where the real-time measurements are taken. This is due to the increase in people activity in the areas. Due to this, FNR increases for LS-SVM. Moreover, the proposed rule-based classifier achieves true classification rate of 97% which is equal to $(1 - P_T) \times 100$.

Chapter 4

4.5.2. Range Mitigation Performance

The performance of the proposed range algorithm for 1200 measurements in two different scenarios is provided in Table 4.4. In each scenario, measurements are taken at three different locations (i.e. T_1 , T_2 , and T_3) as depicted in Fig. 4.1. In Table 4.4, the performance of the range mitigated algorithm is measured in terms of percentage error (ϵ_{Mit}), and range improvement factor (δ_{imp}). ϵ_{Mit} is the percent error of $R_{Mit.}$ (i.e., mitigated range) relative to R_{true} (i.e., true range), and, δ_{imp} is the percent error improvement in range error ($R_{Mit.}$) resulting from the mitigation algorithm over the NLOS range measurement($R_{NLOS.}$), in relation to the R_{true} .

The average δ_{imp} for the office and warehouse are 5.65%, and 5.68%, respectively. An overall average of these values yields a δ_{imp} of 5.66%. It is observed that δ_{imp} is improved considerably where there is severe NLOS as in the case of R_2 ranging at T_1 position in all scenarios. This is due to ranging error around 1 m in the case. From Table 4.4, it can be seen that ϵ_{Mit} is low for most of the measurements due to less difference between $R_{Mit.}$ and R_{true} which shows the effectiveness of the proposed ranging algorithm.

4.5.3. Localization performance

The performance of the localization algorithm from Section 2.71 using mitigated ranges and NLOS ranges is determined in terms of position improvement factor (PIF) which is $\frac{d_{NLOS}}{d_{Mitigated}}$ ratio. The ratio is between NLOS distance (d_{NLOS}) (i.e., the difference between true LOS position and NLOS

Table 4.4: Range Mitigated & NLOS performance

N= 1200		Office		Warehouse	
		ϵ_{Mit} (%)	δ_{imp}	ϵ_{Mit} (%)	δ_{imp} (%)
Position T_1	R_0	0.91	2.37	1.90	6.18
	R_1	2.32	2.24	4.47	4.91
	R_2	3.73	15.31	0.84	5.08
Position T_2	R_0	1.34	3.94	0.63	5.70
	R_1	2.76	2.35	0.56	4.98
	R_2	0.42	5.66	0.24	8.30
Position T_3	R_0	0.63	5.70	0.29	4.59
	R_1	0.56	4.98	3.04	1.99
	R_2	0.24	8.30	3.09	9.35

Chapter 4

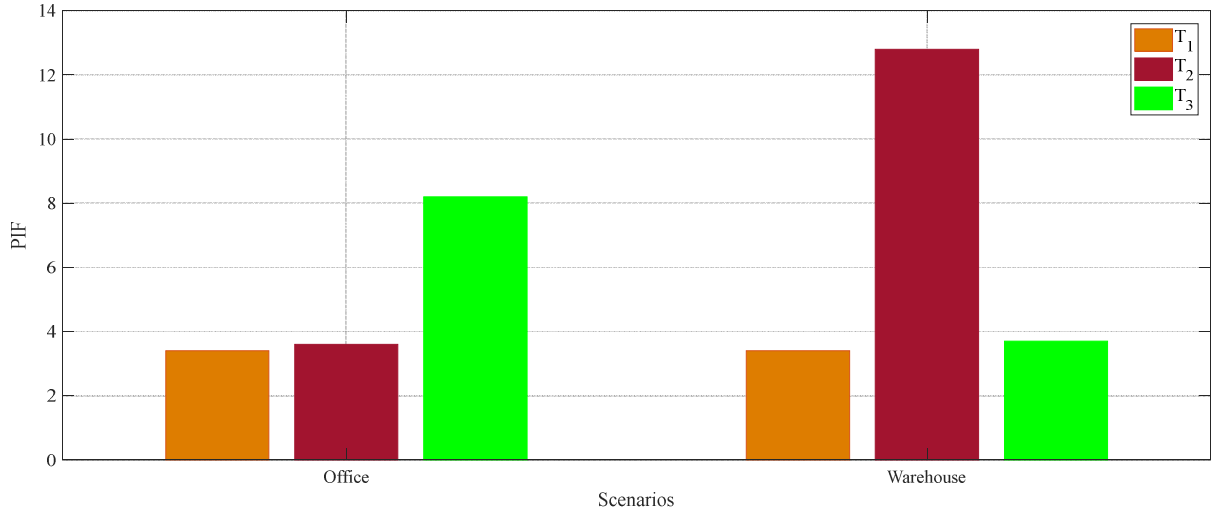


Fig. 4.4: Localization Performance in terms of PIF

position) and mitigated distance ($d_{Mitigated}$) (i.e., the difference between true LOS position and mitigated distance position). The distances are computed as:

$$d_{NLOS} = \sqrt{(x_{T_iLOS} - x_{T_iNLOS})^2 + (y_{T_iLOS} - y_{T_iNLOS})^2} \quad (4.13)$$

$$d_{Mitigated} = \sqrt{(x_{T_iLOS} - x_{T_iMitigated})^2 + (y_{T_iLOS} - y_{T_iMitigated})^2} \quad (4.14)$$

The PIF is computed for each of the position (i.e., T_1 , T_2 and T_3) in all the scenarios. The average of PIF for each of the position in a particular scenario are illustrated in Fig. 4.4. From Fig. 4.4, it can be deduced that the PIF varies from 3.42 to 12.5054. This variation in PIF value is due to different channels experiencing NLOS with varying severities. For instance, a low PIF is due to a

Chapter 4

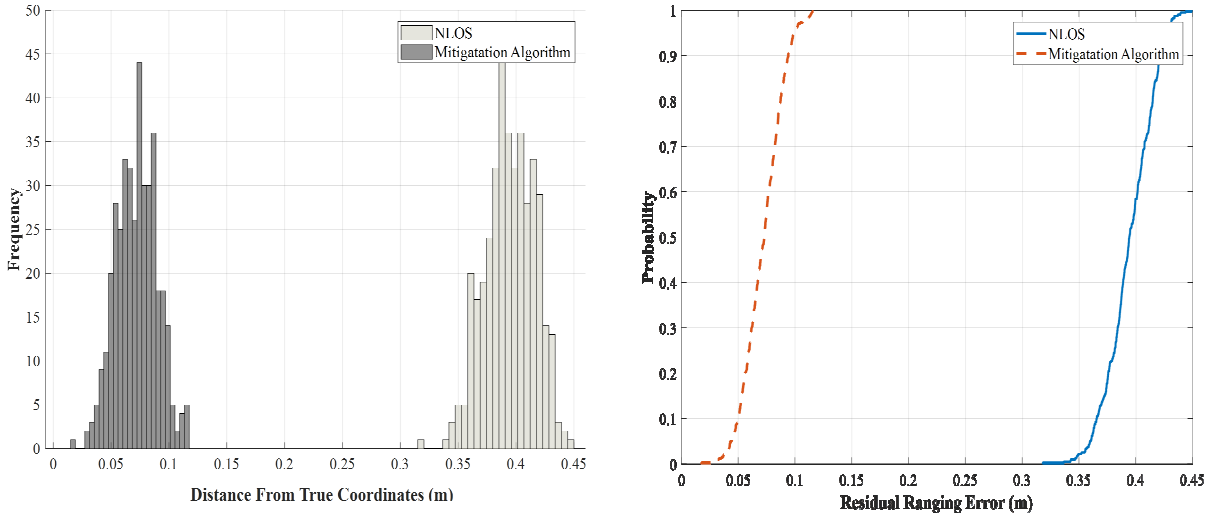


Fig. 4.5: Histogram & CDF of NLOS & Mitigated Algorithm ranges

mild severity of the encountered NLOS. Accordingly, If the NLOS range measurements were only slightly greater (i.e., due to the severity) than the actual LOS range measurements, the PIF will be lower as the margin of the ranging error is lower.

The effectiveness of range mitigation algorithm is gauged from PIF factor as shown in Fig. 4.4. The large PIF number shows that there is a significant difference between mitigated distance and NLOS distance. The difference in the distances is also shown from CDF and histograms in Fig. 4.5. The CDF also shows that the overall error decreases by 0.35 meter for the mitigated technique compared to NLOS condition.

4.6. Summary

In this chapter, a novel rule-based classification technique to identify LOS/NLOS and geometric-based range mitigation are developed. Moreover, a probabilistic model, for the non-industrial environment to show one anchor-agent pair in the set of three is most likely in NLOS condition, is presented. The (proposed) classifier and range mitigation algorithm are validated using experimental measurements in two different environments. The experimental study has shown that the proposed classifier can achieve 97% success rate in identifying LOS/NLOS. In addition, the performance of the proposed ranging algorithm is quantified in terms of percentage mitigated error, percentage improvement range factor and position improvement factor. The ranging error shows lower error up to 4.47% along with improvement range factor of 10.47% compared with

Chapter 4

NLOS ranging. The position factor shows an improvement of up to 12 times compared with position using an unmitigated NLOS range. The standard deviation of the mitigation results is lower than that attained by a system running no correction algorithm. Moreover, the standard deviation of our proposed mitigated solution is 0.2517 m less than the NLOS solution on average, across all the test rooms.

As a next step (which is provided in Chapter 5), NLOS mitigation is extended for scenarios where two or all of the agent anchor's pairs are in NLOS. Moreover, the rules for identifying LOS and NLOS are expanded for fuzzification and estimating ranging error bias based on the severity of NLOS conditions. The biased value is subtracted from the estimated range to estimate mitigated range for enhancing position accuracy of the system where more than one anchor-agent pair are in NLOS.

RULE BASED RANGING ERROR MITIGATION FOR IR-UWB: A FUZZY LOGIC APPROACH

5.1. Introduction

Fuzzy logic is categorized as a soft computing method which accommodates the uncertainties of the real world. In a more specific sense, fuzzy logic is an extension of multivalued reasoning whose objective is to do estimated reasoning rather than the strict solution. It achieves robustness, tractability, and low-cost solution by exploiting the tolerance for imprecision, partial truth and uncertainty in measurements. In contrast to the traditional hard computing where Crisp logic is applied, Fuzzy logic may have true or false values with a degree of certainty or uncertainty. Furthermore, Fuzzy Logic is close to the human way of reasoning which finds a way in many control and classification applications [73]. Particularly, in the wireless domain, Fuzzy Logic has gained popularity for classification and clustering applications in recent years due to low cost and less computational complexity burden [74, 75]. In this chapter, Fuzzy logic is applied to CIR parameters to estimate the ranging error and mitigate the error in LOS and NLOS estimated ranges for indoor tracking and navigation (ITN) application domain. Due to ITN's stringent computational complexity and ranging acquisition delay requirements, fuzzy logic solution aligns well with the requirements. Moreover, measurements uncertainties are covered optimally by the fuzzy approach [76, 77]. Estimation (or mitigation) of the error is done in one step rather than in two (i.e., the first classification of LOS or NLOS, and second, mitigation of NLOS errors). Moreover, ranging errors in LOS condition due to multipath propagation is also accounted for and corrected in the proposed range mitigation technique based on fuzzy logic.

In this chapter, first, basic terminologies of Fuzzy Logic is described. Second, uncertainties in CIR parameters (i.e., received signal strength, first path signal strength and rise time) due to LOS and NLOS are modeled. The ranging errors related to the uncertainties is analyzed. The theoretical analysis is the foundation and served as expert knowledge for designing the rule inference mechanism and a fuzzy inference system (FIS). Third, the proposed FIS model is presented. Fourth, measured parameters are compared with the theoretical uncertainty analysis. The

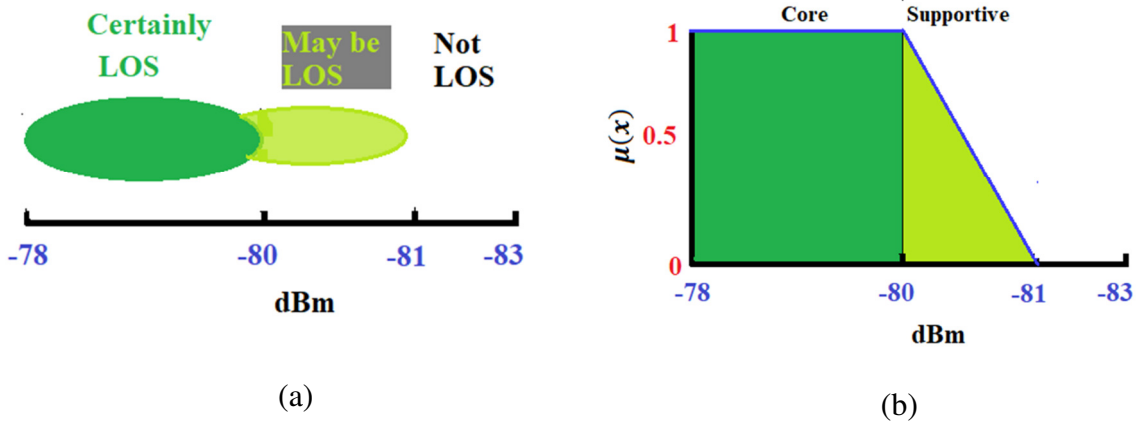


Fig. 5.1: Fuzzy classification & membership function (a) classification. (b) membership function

comparison is supportive in designing of the membership functions of the FIS system. Finally, the experimental evaluation of the proposed system and localization performance are presented.

5.2. Fuzzy Terminologies

5.2.1. Fuzzy Set

In classical theory, elements are classified into different sets based on Boolean logic, i.e., either an element belongs to a particular set or not. However, in fuzzy theory, an element belongs to a particular set or not with the degree of membership function between 0 and 1. Logically 0 interpreted as completely not a member and 1 as an absolute member., A fuzzy set which describes a condition of LOS based on received signal strength, where reading is greater than -80 dBm has defined criteria for an element to belong to a set of LOS with a full degree of membership. In the case, a reading of -78 dBm which has a full degree of membership Aas illustrated in Fig. 5.1(a). However, a reading of -83 dBm is far away from the criterion and does not belong to the set. Another reading of -81dBm is close to the criterion, and it is reasonable to categorize to LOS set with a partial degree of membership, and the value of membership depends on the features of the membership function.

5.2.2. Membership Function

A shape or curve that defines the features of a fuzzy set is called a membership function (MF). It assigned each element to corresponding membership value or degree of membership in close internal $[0,1]$. It has a core area and supportive boundaries as shown in Fig. 5.1(b). An input variable x and the corresponding degree of membership $\mu(x)$ are defines on horizontal and vertical axes respectively. A full degree of membership is represented by the core region and $\mu(x) = 1$. Supportive region where $1 > \mu(x) > 0$ covers the fuzziness and tells the degree of certainty that a particular value of x belongs to a fuzzy set. Generally, there are five curves (or MFs) used which are Trapezoidal, Triangle, Gaussian, Sigmoidal, and Generalized Bell. Generally, Gaussian or Triangle MFs are used [76, 77].

5.2.3. Fuzzification

In fuzzy logic, a process of converting numerical input values into a linguistic variable with a certain degree of membership is called fuzzification. The process of mapping input space onto linguistic variable is done using fuzzy set and corresponding MF. Usually, more than one MF are used to map the signal input onto multiple linguistic variables. Fuzzification process facilitates a fuzzy inference mechanism to be applied to the input variable(s).

5.2.4. Fuzzy Inference

A process of projecting input variable(s) onto output space through rules structure is called fuzzy inference. The structure is parallel If-Then as illustrated in Fig. 5.2. A single If-Then rule is of the following form:

$$\text{IF } x \text{ is low, THEN } y \text{ is low,} \quad (5.1)$$

The L.H.S. of the rule in (5.1), where input(s) is located, is called antecedent. The R.H.S., where the output is located, is called consequent. Multiple inputs are connected using fuzzy logic operators. The operators are AND, OR and NOT. The AND operation is interpreted as min function, i.e., $\min(x_1, x_2)$. OR operation interpreted as a max function, thus $x_1 \text{ OR } x_2$ is equivalent to a $\max(x_1, x_2)$. And NOT x_1 becomes $1-x_1$.

The rules are designed thru expert knowledge of a particular process within an application. There are three types of fuzzy inference mechanism namely Mamdani, Surgeno, and Takagi-Sugeno-Kang (TSK) [76]. The three types differ from each other at the output after the inference

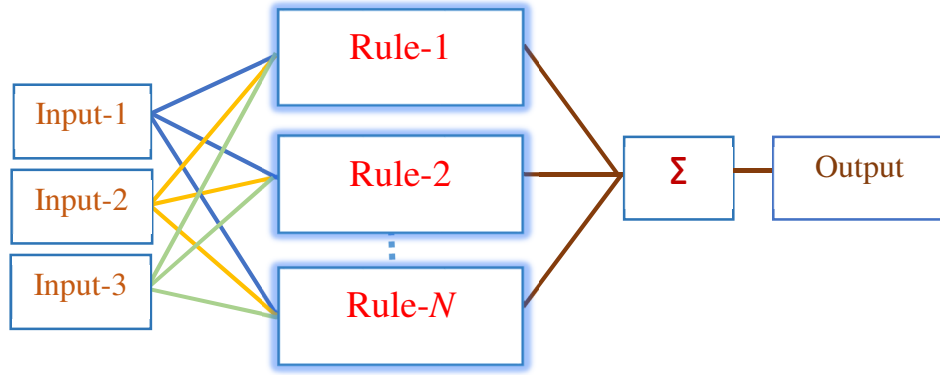


Fig. 5.2: Rules Structure

mechanism. Mamdani output is a linguistic variable, whereas Surgeno output is a numerical number [76]. TSK is a hybrid form of Mamdani and Surgeno [76]. For most classification problems, Mamdani is commonly used as it is ease to design and resembles human analogy for inference and control [76]. In this work, Mamdani is used. Moreover, Mamdani requires a defuzzification process to convert a linguistic variable into a numerical value at the output.

5.2.5. Defuzzification

A process of converting a linguistic variable into crisp value after rule inference is called defuzzification. There are four types of defuzzification namely, mean of max (MoM), center of gravity (GoC), height method (HM), and look up table [77]. GoC method is commonly used in many applications [77].

5.3. Parameters Uncertainty Analysis

In this section, uncertainties in the CIR parameters due to LOS and NLOS conditions are discussed. Moreover, ranging error, correlation to the uncertainties, is considered.

The CIR parameters are RSS, FPPS and rise time RT.

5.3.1. Received Signal Strength (RSS)

It is known that RSS, transmitted power, and the distance between transmitter and receiver are correlated to each other by well-known Ferris equation [45]. In addition, RSS is affected by

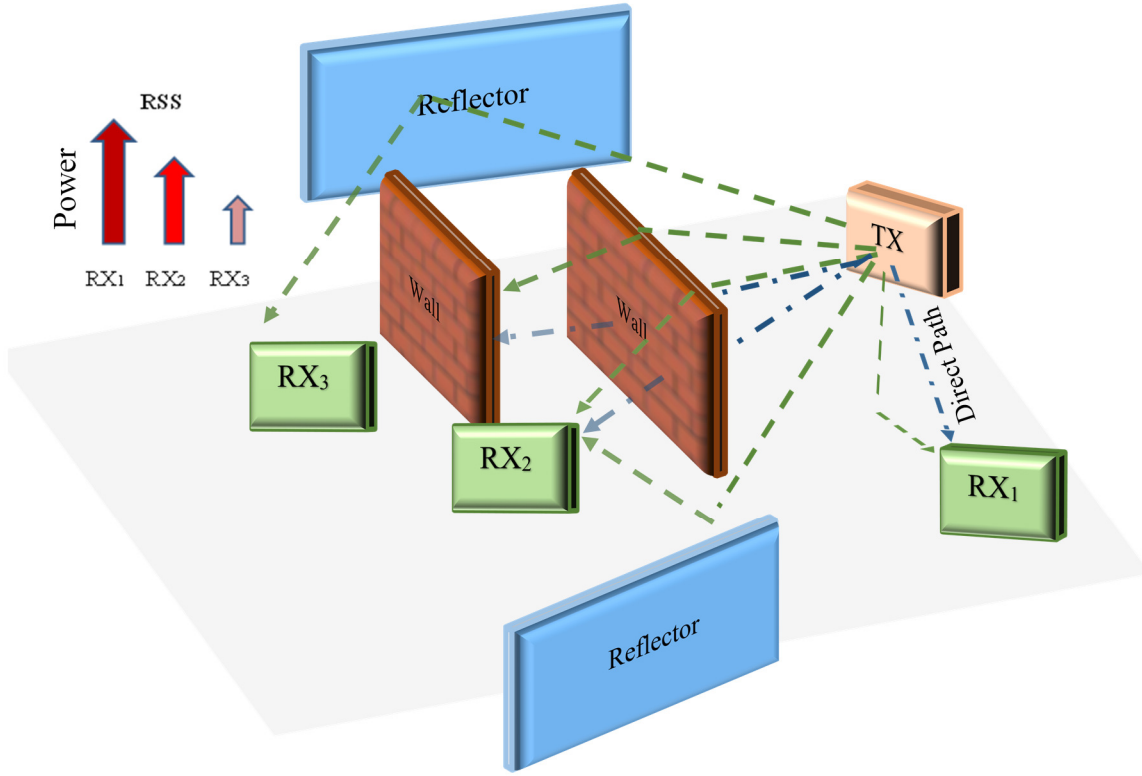


Fig. 5.3: RSS and LOS/NLOS

multipath propagation components (MPCs) and condition of the channel (LOS or NLOS) as illustrated in Fig. 5.3. In the Figure, it is assumed that TX power to all RXs is equal and all RXs are at the same distance. So, RX1 received max power related to transmitted power due to LOS, RX2 received less power than RX1 due to NLOS, and RX3 received the least power compared to RX1 and RX2 due to severe NLOS. The instantaneous RSS varies due to MPCs and LOS/NLOS conditions, can be modeled as:

$$RSS_{inst.} = \begin{cases} RSS_{mean} + L & N = 0 (LOS) \\ RSS_{mean} + L + N & N < 0 (NLOS) \end{cases}, \quad (5.2)$$

where L is MPP factor in dBs and N is an attenuation factor in dBs. The N varies with the severity of NLOS. For less severe NLOS condition, N is low, and RSS is high. However, for very severe NLOS condition, the N is high and RSS is low. For the LOS condition, RSS is very high.

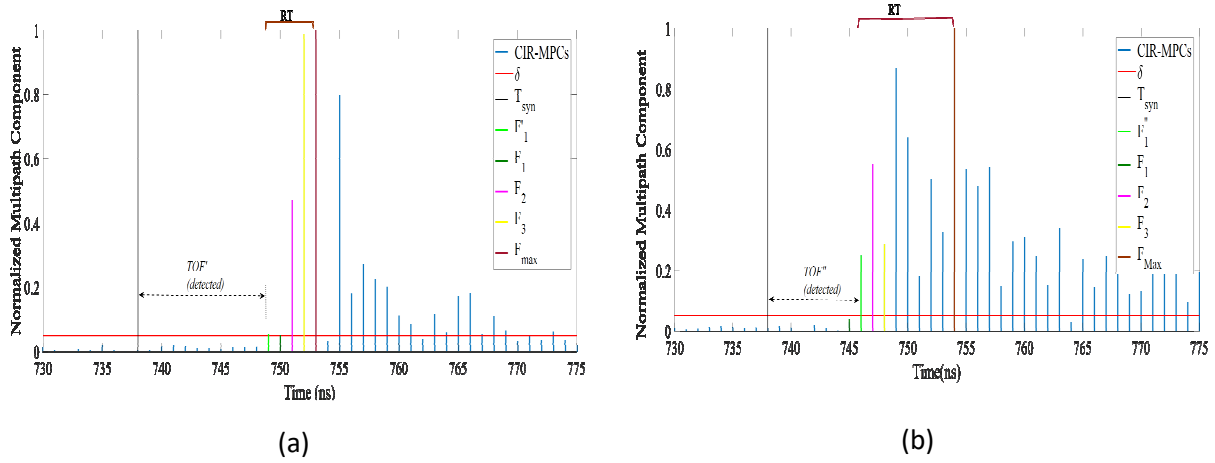


Fig 5.4: CIR in LOS and NLOS (a) LOS (b) NLOS

5.3.2. First Path Power Strength (FPPS)

In IR-UWB, the FPPS is estimated using CIR leading edge MPC (F_1) followed by two MPCs in CIR (F_2 and F_3) as illustrated in Fig. 5.4 [1]. For ranging estimation, leading edge detection (LED) algorithm is employed to detect F_1 based on time of arrival (ToA) technique. Therefore, FPPS is a vital indicator in IR-UWB. Similar to RSS, FPPS varies due to MPCs and the channel condition. Therefore, FPPS can be modelled as follows:

$$FPPS_{inst} = \begin{cases} FPPS_{mean} + L_{FP} & N_{FP} = 0 \text{ (LOS)} \\ FPPS_{mean} + L_{FP} + N_{FP} & N_{FP} < 0 \text{ (NLOS)}, \end{cases} \quad (5.3)$$

where first path L_{FP} MPP factor in dB and N_{FP} is the first path attenuation factor in dB. The magnitude of N_{FP} is depend on obstruction material and number of obstructions in NLOS conditions. As $RSS_{inst.}$ and $FPPS_{inst.}$ are estimated using CIR magnitude. Hence they are interlinked with each other.

5.3.3. Rise time (RT)

RT is defined as the difference between the time occurrence of F_1 $T(F_1)$ and time occurrence of max MPC (F_{max}) $T(F_{max})$ as given:

$$RT = T(F_{max}) - T(F_1), \quad (5.4)$$

RT varies according to the condition as demonstrated in Fig. 5.4. The Figure shows that RT in LOS is low while it is high in NLOS.

Chapter 5

5.3.4. Ranging error

In this subsection, the relationship between ranging error and FPPS (as well as RSS) is developed. For the LED algorithm, the first MPC above the threshold is considered as the first path [1]. Based on that, the distance between the TX and RX is estimated as:

$$T_{TOF} = T(F_1) - T_{syn}, \quad (5.5)$$

$$D = T_{TOF} \cdot C, \quad (5.6)$$

where T_{TOF} is the time of flight; T_{syn} is the time at which TX and RX are synchronized; $T(F_1)$ is the time at which F_1 (leading edge magnitude) detected, provided:

$$F_1 > \delta, \quad (5.7)$$

where δ is the threshold level for ToA based estimator (receiver). However, F_1 depends on the received power and channel condition. Moreover, the ranging error depends on detection scenarios of F_1 such as early detection and post detection.

- **Case I (Early detection):**

Consider that leading edge is detected earlier than the true F_1 as shown in Fig. 5.4(a). and denoted by F'_1 . The new TOF' is computed as:

$$TOF' = T(F'_1) - T_{synch}, \quad (5.8)$$

Such that:

$$T(F'_1) < T(F_1), \quad (5.9)$$

$$\Delta T = T(F'_1) - T(F_1), \quad (5.10)$$

Error in the distance is given by:

$$e = \Delta T \cdot C \quad (5.11)$$

From (5.11), the estimated distance is shorter than the true distance and ranging error is negative.

From (5.3) and (5.11), the ranging error depends on the RSS and FPPS power levels.

- **Case II (post detection):**

It is the case where the NLOS condition is present. In this case, the leading edge is detected after F_1 as shown in Fig. 5.4(b). and denoted by F''_1 . TOF' is estimated using (5.8). However,

$$T(F''_1) > T(F_1), \quad (5.12)$$

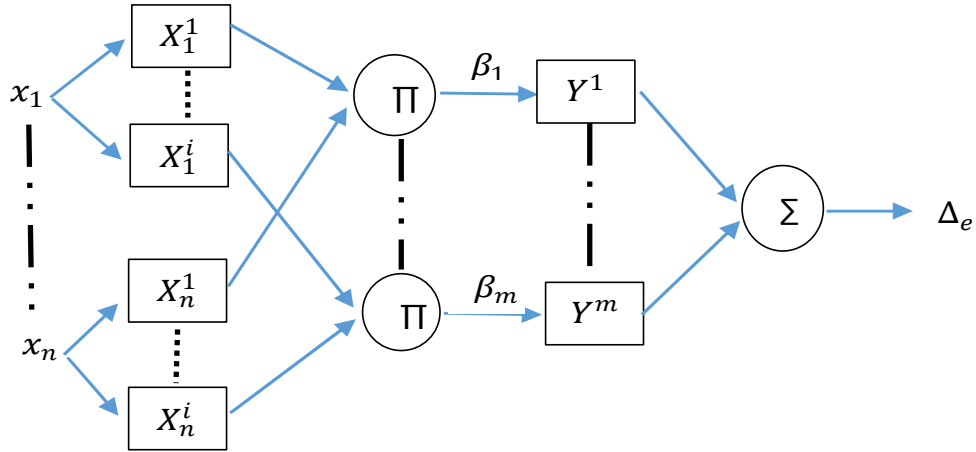


Fig. 5.5: FIS Model

using (5.10), ΔT is positive. Hence error is positive and the error magnitude is correlated with the received FPPS and RSS magnitudes and the magnitudes are related to NLOS severity as in (5.2) and (5.3).

5.4. Fuzzy Inference System (FIS) Model

The parameters' uncertainties and their correlation to ranging error are a mirror to the channel condition (i.e., LOS or NLOS) and severity of the NLOS condition as shown in the preceding section. To overcome the ranging error due to these uncertainties, FIS is presented in this section. In particular, Mamdani multiple input single output (MISO) FIS can be written as:

$$\varphi(r_i) = \beta(r_i) + y, \quad (5.13)$$

where φ is the fuzzified weight of the particular rule r_i , $\beta(r_i)$ is the firing strength of the rule and y is the area of the consequent membership function (MF) of r_i .

$$Z = \frac{\int \mu_Y(y) y dy}{\int \mu_Y(y) dy}, \quad (5.14)$$

where $\mu_Y(y)$ is the output membership function (MF) of output y . According to (5.13) and (5.14), Mamdani multiple inputs single output (MISO) FIS can be depicted as in Fig. 5.5.

where $n \in \{1,2,3\}$ are the number of inputs, i is the total number of MFs, and m is the number of rules, while X_n^i and Y^m are input and output fuzzy sets respectively. Mamdani FIS consist of five steps (or layers) that can estimate output from inputs. Each step output is described as follows:

Chapter 5

- **Step 1: Fuzzification step**

$$S_{1,a,b} = \mu_{x_a^b}(x_a), \quad (5.15)$$

where $a = 1, \dots, n$ and $b = 1, \dots, i$ associated with each input. The antecedent MF is a Gaussian function as it gives the best performance among different membership functions [27].

$$\mu_{x_a^b}(x_a) = \exp \left\{ - \left(\frac{x_a - \gamma_{ab}}{\vartheta_{ab}} \right)^2 \right\}, \quad (5.16)$$

where γ_{ab} and ϑ_{ab} are the parameters referred to as input premise (Gaussian) parameters.

- **Step 2: Inference or rule step**

$$S_{2,i} = \beta_i = \mu_{x_1^i}(x_1) \times \mu_{x_2^i}(x_2) \times \dots \times \mu_{x_n^i}(x_n), \quad (5.17)$$

where $i = 1, \dots, m$. Firing strength β_i of the particular rule is generated using the product (AND) method [76].

- **Step 3: Implication step**

$$S_{3,i} = \beta_i \circ \mu_{y^i}(y^i), \quad (5.18)$$

where $i = 1, \dots, m$. Implication operator is a product. Similar to antecedent MF, consequent MF ($\mu_{y^i}(y^i)$) is also Gaussian function:

$$\mu_{y^i}(y^i) = \exp \left\{ - \left(\frac{y^i - \alpha_i}{\rho_i} \right)^2 \right\}, \quad (5.19)$$

where α_i and ρ_i are the parameters referred to as output premise (Gaussian) parameters.

- **Step 4: aggregation step**

$$S_4 = \sum_{i=1}^m \beta_i \circ \mu_{y^i}(y^i), \quad (5.20)$$

- **Step 5: defuzzification step**

$$S_5 = \Delta_e = Z \circ S_4, \quad (5.21)$$

The crisp output Δ_e is estimated with the defuzzification method (Z) centroid [76].

5.5. Experimental Evaluation

The purpose of the experimental studies is twofold. First, empirically analyze of the measured parameters is presented and compared with theoretical analysis of the CIR parameters'

Chapter 5

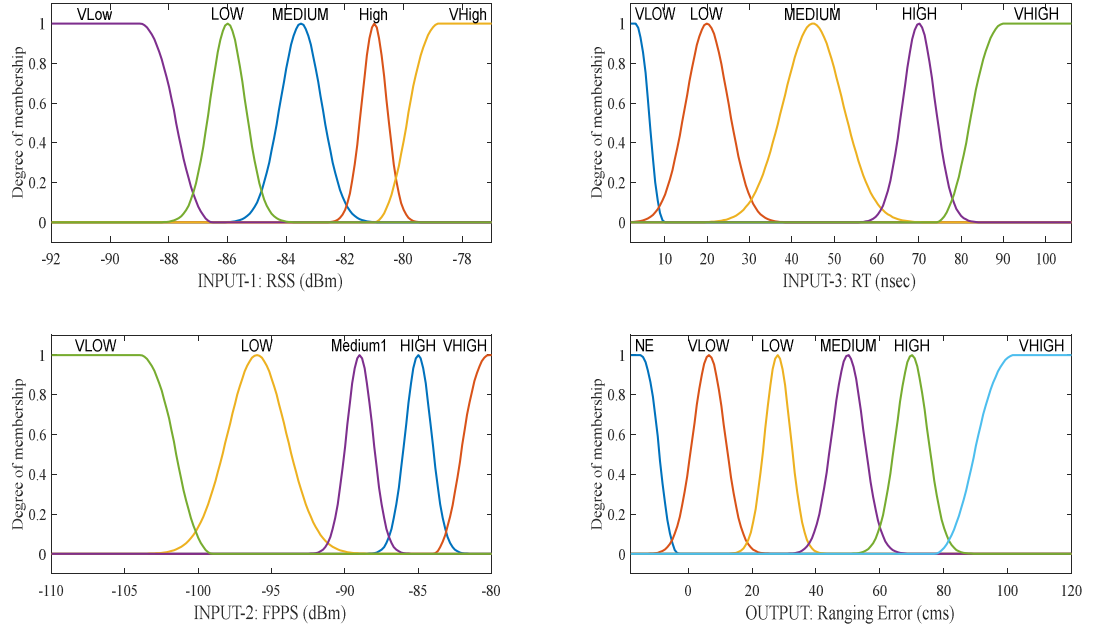


Fig. 5.6: Inputs & outputs MFs for FIS model

uncertainties presented in Section-5.3. The analyses are supportive in designing the FIS model parameters and rules. Second, evaluate the performance of the FIS model to estimate the ranging error in real time environment as presented in Section-5.4. In these experiments, waveforms, range measurements, channel data, received and first path signals' levels, for LOS and NLOS conditions are collected in different scenarios and environments as described in Chapter 3.

5.5.1. Empirical Parameters Analysis

We analyze the measured parameters (i.e., RSS and FPPS levels, RT and ranging errors) based on the theoretical uncertainties analysis of the parameters presented in Section-5.3. From the measurements, we observe that for LOS condition in all scenarios, the RSS is in the range of -78 to -80 dBm and FPPS is in the range of and -80 to -82 dBm. We labeled the ranges as very high. For mild NLOS condition, the RSS is in the range of -80 to -82 dBm and FPPS is in the range of -82 to -86 dBm. We labeled the ranges as high. Subsequently, as the NLOS severity increases, we labeled the ranges as a medium, low, and very low for RSS and FPPS as shown in Fig. 5.6. From the observations, we find that RSS and FPPS levels are very high in LOS scenarios and degrade gradually as the NLOS severity increases and the relationship confirms the theoretical analysis.

Chapter 5

Similarly, we find that RT is in the range of 3-4 nsec. for all the scenarios in LOS condition. We labeled the range as very low. This is due to strongest path presented after leading edge in LOS scenarios. For mild NLOS condition, RT is in the range of 5-10 nsec. and it is labeled as low. As the NLOS severity increases, the RT increases and the ranges are labeled as medium, high, and very high accordingly as illustrated in Fig. 5.6.

For LOS condition, we find that ranging errors are in the ranges of -15 to -2 cm, we labeled the ranges as negative (NE). The errors can be negative as discussed in Case 1 in Section-5.3. For mild NLOS conditions, the ranging error is in the range of 2 to 12 cm and labeled as very low (V. Low). However, as the severity of the NLOS condition increases the ranging error magnitude increases, and the ranges are labeled as low medium and high as shown in Fig. 5.6. The parameters empirical comparison and theoretical analysis of the parameters uncertainties are supportive in designing the input and output MFs using (14) and (17), respectively and as shown in Fig. 5.6 as well as designing of FIS rules as provided in Table 5.1.

5.5.2. Ranging Error Mitigation Performance

For two different MFs (i.e., Gaussian and Triangle) and two different defuzzification processes (i.e., GoC and MoM), the FIS model performances for estimating the ranging error are illustrated in Fig. 5.7. The performance is quantified in terms of probability density function of residual

Table 5.1: Rules for FIS

S. No.	Antecedent			Consequent
	RSS	FPPS	RT	Ranging Error
1	V. High	V. High	V. Low	V. Low
2	V. High	High	V. Low	V. Low
3	V. High	Medium	LOW	N.E
4	High	High	V. Low	V. Low
5	High	Medium	Low	N.E
6	High	Low	Medium	Low
7	High	V. Low	Medium	Medium
8	Medium	Medium	V. Low	V. Low
9	Medium	Low	Low	N.E
10	Medium	V. Low	Low	Medium
11	Low	Medium	V. Low	High
12	Low	Low	Low	V. High
13	Low	V. Low	Medium	V. High
14	V. Low	Low	V. Low	High
15	V. Low	V. Low	Low	V. High

Chapter 5

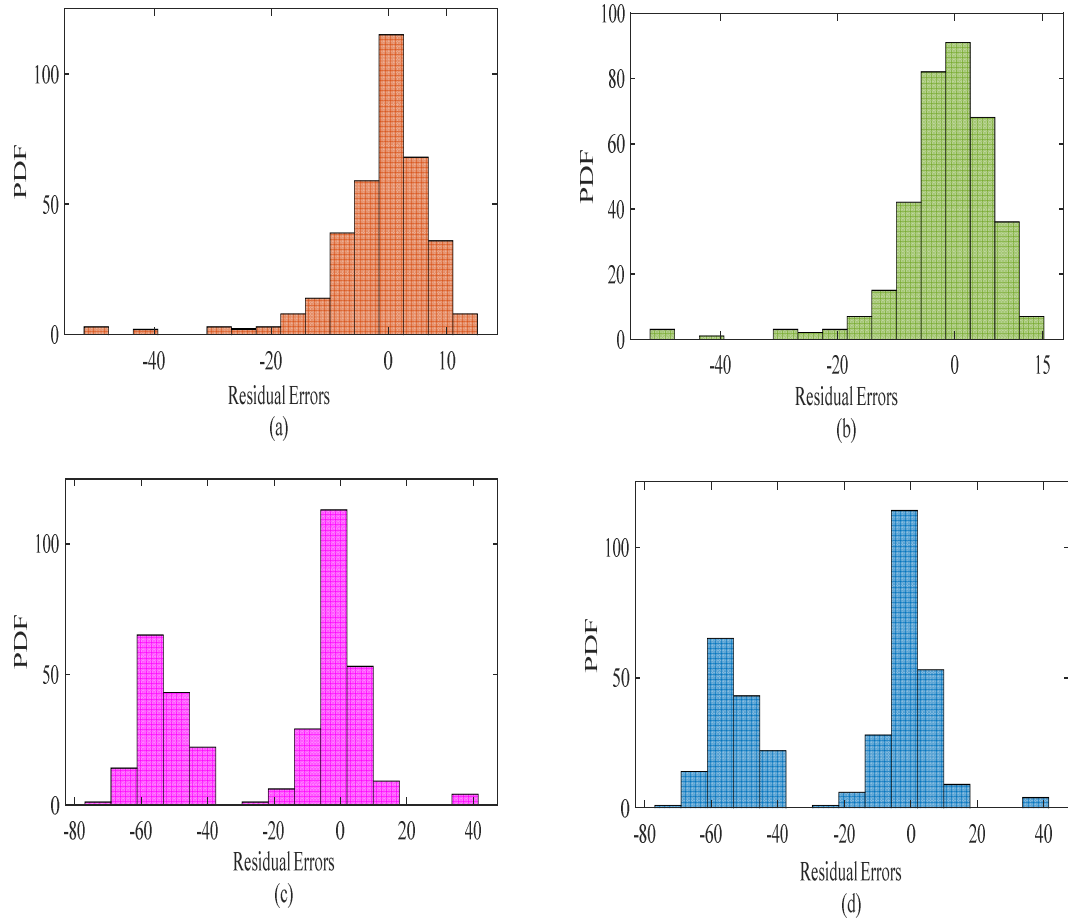


Fig. 5.7: Performance evaluation for different MFs and defuzzification processes: (a) Combination-I (b) Combination-II (c) Combination-III (d) Combination-IV

ranging errors, (i.e., errors remaining after mitigation). From Fig. 5.7(a), it can be deduced that residual errors are concentrated around zero for Gaussian MF along with GoC defuzzification (Combination-I). The performance of Gaussian MFs and MoM defuzzification combination (Combination-II) is quite similar to the combination-1. However, the residual errors are concentrated more on the negative side as depicted in Fig. 5.7(b). The performance degrades when using Triangle MFs irrespective of the defuzzification process used as illustrated in Fig. 5.8.c & Fig. 5.8.d for Triangle MF and GoC defuzzification (Combination-III) and Triangle MF and MoM defuzzification (Combination-IV) respectively. So, Combination-I would be considered from thereon.

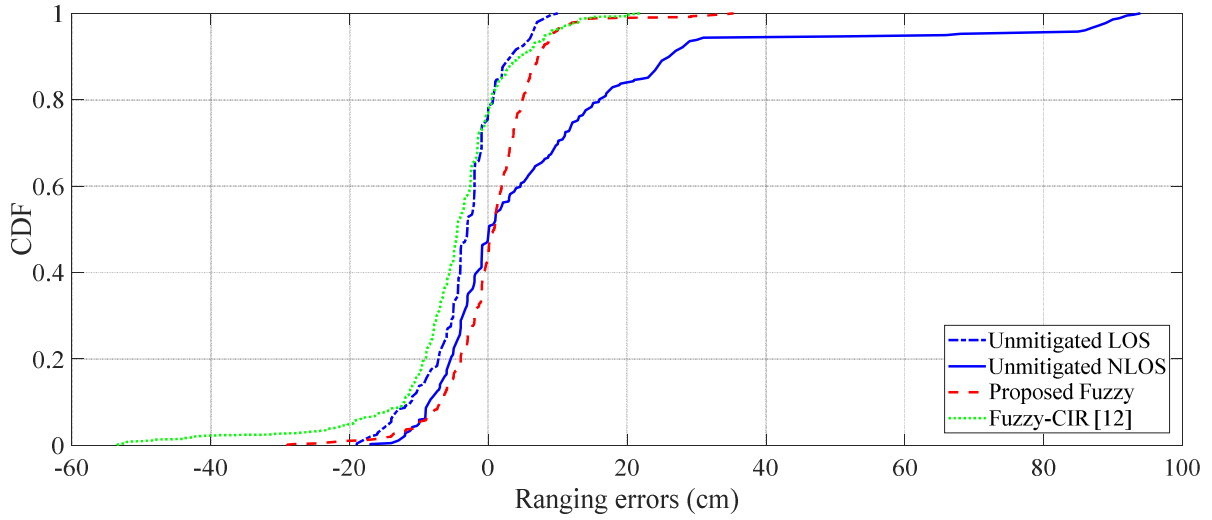


Fig. 5.8: CDF for residual ranging errors.

The fuzzy mitigation ranging performance is quantified in terms of residual ranging errors and compared with unmitigated LOS, and NLOS ranges as shown in Fig. 5.8.

Fig. 5.8 demonstrates the CDF of the residual errors for the proposed fuzzy system along with existing work from [12] and unmitigated LOS and NLOS errors. For a fair comparison with existing from [12] labeled as Fuzzy-CIR (as it depends on frame length CIR data), we estimated parameters (i.e., SNR, RMS delay spread, kurtosis, and skewness) from experimentally collected CIR data. In Decawave® devices, for the suggested optimum threshold level (δ) [1], ranging errors are more on the negative side within -10 cm for most of the readings. Moreover, in some experimental setups where the estimated range is more than 10 m, ranging errors spread to -20 cm as observed in Fig. 5.8. This is also observed for some SNLOS cases where the strong path is the first path followed by weak MPCs in CIR. We considered ranging errors in LOS and SNLOS conditions and estimated ranging errors based on RSS, FPPS and RT levels in these conditions. However, Fuzzy-CIR does not consider LOS and SNLOS ranging errors. Moreover, in propagation conditions where metal obstructions and more MPCs in CIRs are presented and observed ranging errors are not that high (less than 20 cm). For these conditions, Fuzzy-CIR estimated large errors (between -20 and -40 cm). This is observed for less than 6% of the readings as shown in Fig. 5.8. It is due to higher estimated RMS delay spread. Whereas for the proposed fuzzy system, RSS and

Chapter 5

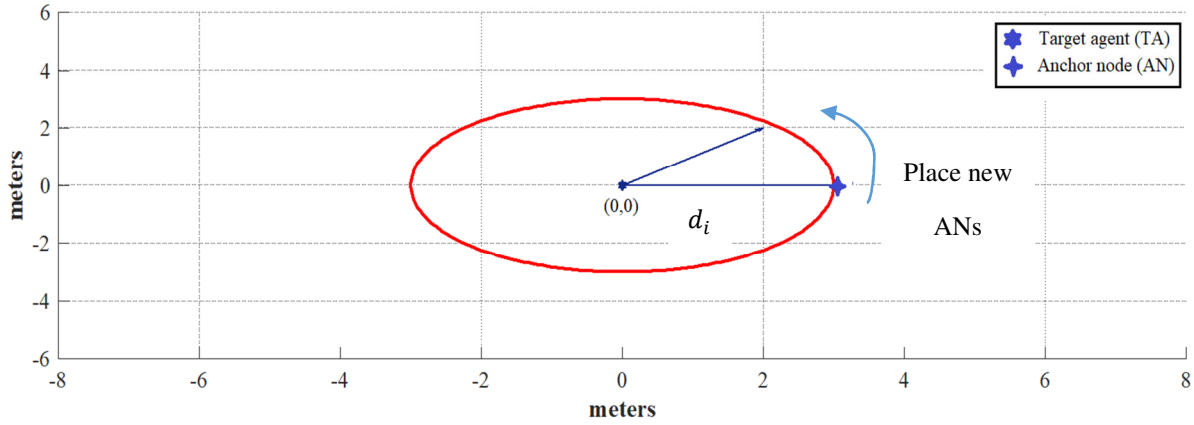


Fig. 5.9: Anchors Placement around Target node with different d_i according to (5.22)

FPSS levels are in the high or mid ranges (as stated above) and due to this range error estimation are minimal (less than -15 cm.) for the conditions. For higher errors in NLOS conditions (>25 cm) both systems (i.e., proposed and Fuzzy-CIR) are performed identical as shown in Fig. 5.8. However, for Fuzzy-CIR, the parameters' estimation need frame length CIR data which add latency in estimating range and ranging errors. Whereas this is not the case for the proposed Fuzzy system. Moreover, for residual errors with $\pm 10\text{cm}$, from Fig 5.8 we have CDF=90.97% for the proposed fuzzy system compared with CDF=79.87% Fuzzy-CIR system and CDF=64.62% for unmitigated NLOS ranges. This shows the ranging performance increment over the Fuzzy-CIR system and NLOS ranges.

Moreover, the computational burden is measured in terms of input-output delay time (T_{IN-OUT}). It is defined as the time taken by fuzzy system to estimate the crisp output provided inputs [41]. For the proposed system and existing work from [12], the average of T_{IN-OUT} with standard deviation is provided in Table 5.2. The statistics is taken using Profile viewer in Matlab® for 21 executions. The T_{IN-OUT} is estimated on Intel Core i5 CPU with clock speed $2.4010 \text{ e}^{-09} \text{ s}$ with installed RAM

Table 5.2: Computational time

Method	$T_{IN-OUT}(\text{ms})$	
	Mean	Std. Deviation
Proposed Fuzzy system	54.7	3.7
CIR-Fuzzy [12]	59.9	5.4

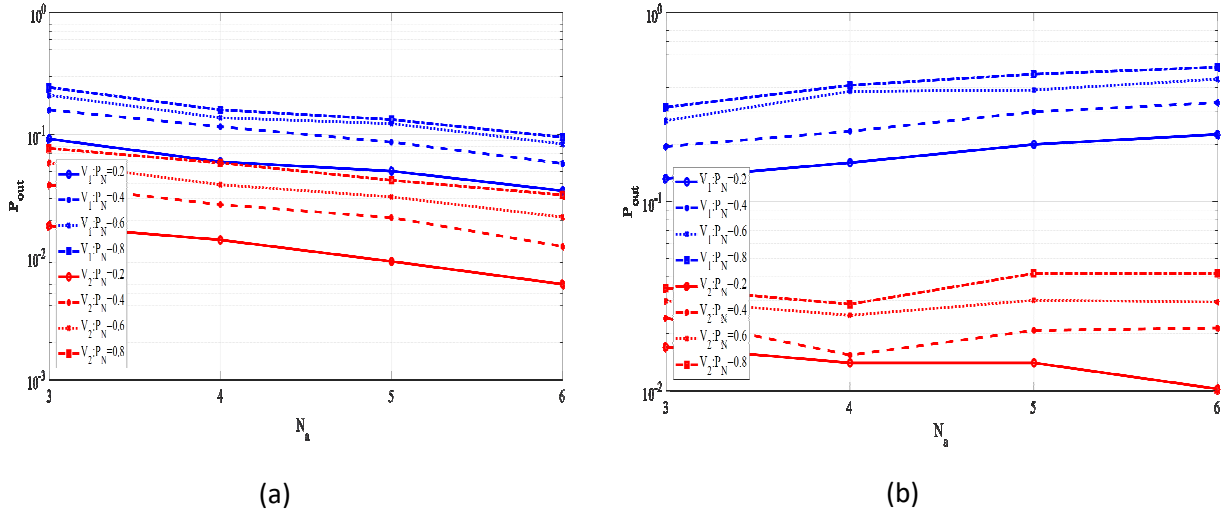


Fig. 5.10: Outage Probability for various N_a with varying P_{NLOS} in: (a) Warehouse; (b) Office

capacity of 8GB. It can be deduced that average T_{IN-OUT} is reduced by 5ms using the proposed fuzzy system for error estimation. Hence the system is putting less computational burden compared to [12].

5.5.3. Localization Performance

The performance of localization is evaluated using fuzzy mitigated ranging. To evaluate the performance, we simulated the localization network using the following settings: anchor nodes (ANs) $3 \leq N_a \leq 6$ with varying probability of NLOS $0.2 \leq P_{NLOS} < 1$. The ANs are placed around the target agent (TA) with true position $P = (0,0)$. For every AN $1 \leq i \leq N_a$, the true distance (d_i) is selected from the pool of scenarios (as discussed in Section-V) associated with the i^{th} scenario and the i^{th} AN is positioned around the agent as illustrated in Fig. 5.9 using:

$$A_i = d_i \left(\cos \left(\frac{2\pi(i-1)}{N_a} \right), \sin \left(\frac{2\pi(i-1)}{N_a} \right) \right), \quad (5.22)$$

From the measurements, the estimated distance between the agent and ANs are used to estimate the position of the agent using (2.2). The i^{th} estimated distance (\hat{d}_i) is drawn from NLOS pool with P_{NLOS} and from LOS pool using $(1 - P_{NLOS})$. Similarly, based on the fuzzy mitigated ranges,

Chapter 5

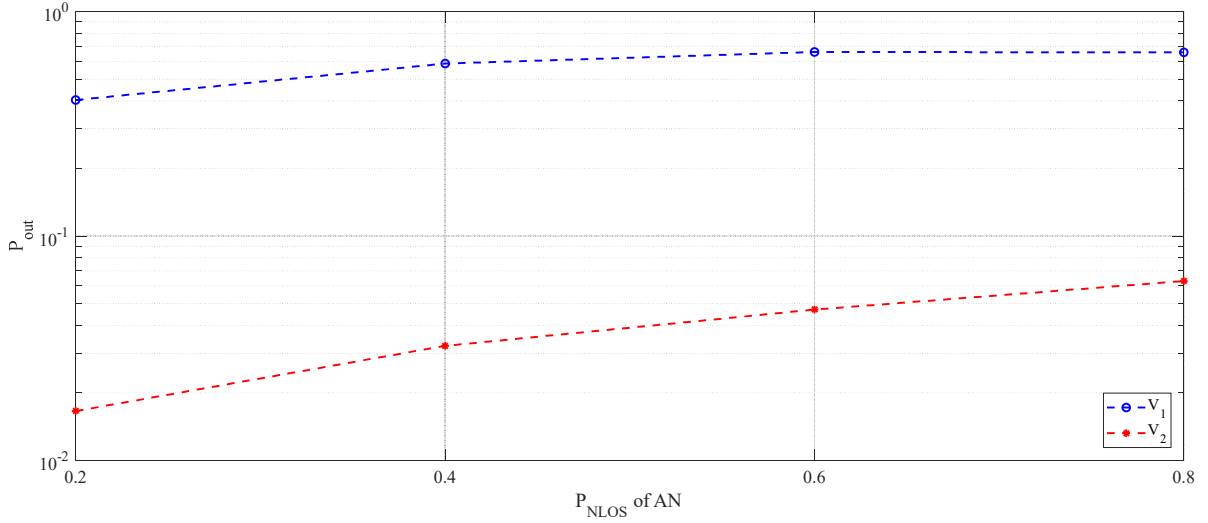


Fig. 5.11: Outage Probability for $N_a = 3$ with varying P_{NLOS} in worst scenarios

the estimated agent position is determined using (1) and the i^{th} fuzzy range (\tilde{d}_i) associated with the scenario is selected for the i^{th} AN.

The reliability of the localization is measured by outage probability (P_{out}). The P_{out} is defined as the probability that the position error is greater than the threshold error as given:

$$P_{out}(e_{th}) = \left\{ \|P - \hat{P}\|_2 > e_{th} \right\}, \quad (5.23)$$

where \hat{P} is the estimated position. We consider threshold error (i.e., $e_{th} = 15$ cm). The P_{out} is determined through Monte Carlo simulation for 5000 networks created using (5.22) and the target agent for each set of N_a . The P_{out} for networks with ANs from 3 to 6 with varying P_{NLOS} for both the environments, namely, warehouse and office, are illustrated in Fig. 5.10. In the Figure, the P_{out} using unmitigated ranges and fuzzy ranges are labelled as V_1 and V_2 , respectively. Moreover, from the Figure, the position errors are low (i.e., less than 10%) for low P_{NLOS} (i.e. 0.2). However, as the uncertainties increases the P_{out} increases. In the case of V_2 , P_{out} is relatively low (i.e., below 10%) even for high P_{NLOS} in both the environments. It is observed that as P_{NLOS} increases, increasing N_a does not helpful in decreasing the P_{out} . It is due to high ranging errors in unmitigated ranges, particularly observed in office environment case as illustrated in Fig. 5.10(b).

Now let us considered for $N_a = 3$ with the worst scenarios from both the environments as shown in Fig. 5.11. The worst case scenarios are defined as the ranging errors vary between 40 and 100

Chapter 5

cm under NLOS condition. From the Figure, the P_{out} , is consistently high for every P_{NLOS} using true ranges. However, P_{out} is considerably low (i.e., less than 10%) for the system using fuzzy ranges (V_2) compared to V_1 . This is due to considerable reduced ranging errors in fuzzy mitigated ranges.

5.6. Summary

Traditionally, statistical and machine learned methods are employed to tackle range errors and enhance the accuracy of localization in IR-UWB. These approaches are adding a delay in position updates and computational burden in indoor tracking and navigation systems. Moreover, machine learning based models are cumbersome to train and specific to the trained scenarios. In this paper, we have proposed to employ fuzzy logic to estimate ranging error and enhance localization accuracy. In addition, the fuzzy mechanism was employed to cope with the errors present in LOS condition due to MPP and blindly estimated the ranging errors. In other words, prior or posterior knowledge of LOS or NLOS conditions is not required. The ranging correction and localization performance are evaluated in terms of the CDF of the residual errors and the outage probability with extensive experimental measurements in indoor environments using IR-UWB devices.

The results showed that the residual errors after fuzzy correction are concentrated around ideal LOS performance (i.e., which has minimal errors). In comparison with Fuzzy-CIR system [12] and NLOS ranges, the proposed ranging error correction shows improvement in CDF of 11% (in comparison with Fuzzy-CIR [12]) and 26% (in comparison with NLOS ranges) for ranging errors with ± 10 cm. Moreover, the simulated localization system using fuzzy corrected ranges showed more robustness against the position errors than the system using unmitigated ranges. Finally, the result facts demonstrated the effectiveness of employing a fuzzy logic approach for ranging errors mitigation in IR-UWB.

6.1. Contributions

This dissertation has presented two methods for enhancing IR-UWB based indoor localization accuracy while reducing delay in estimating the position and computational requirement. The two methods are based on rules, and these rules are designed that utilized CIR parameters. In the first method, classification of LOS and NLOS condition is proposed, and the classification is based on Boolean logic. The logic is based on the rules. After the identification phase, a range error is corrected for NLOS link based on geometric correction algorithm that utilized two LOS ranges to correct one NLOS range in the set of three ranges.

The second method corrects more than one range which utilized rules in the FIS system. The system is based on fuzzy logic whose inputs are CIR parameters and output is estimated error. The error is utilized to correct corrupted range and corrected range(s) which is called mitigated range(s) is utilized to estimate the TN position.

Both the methods are validated using real-time data collected in experimental studies. The studies are carried out in office and warehouse setups in University of Windsor premises using Decawave evaluation kit. In the setups, thirty different scenarios were created that emulate LOS and NLOS conditions using different obstructions.

In the first method, it was shown that using RSS, FPSS and RT parameters reduced delay while achieved low misclassification rate. The proposed classification methodology is compared with [40] and [7] in terms of misclassification rate. The classification method has lower classification rate compared to [40] and [7] while reducing delay and require less computational resources compared to [7]. In addition, the proposed classification does not depend on environment aspect compared to machine learning based classification [7] which requires training data from a particular environment to train the model.

In the second method, fuzzy logic is applied to the variation of RSS, FPSS and RT parameters. The variation is proportional to NLOS severity. Moreover, a relationship is developed between parameters' variation and ranging error. The relationship is utilized as expert-based knowledge for designing of fuzzy mechanism and FIS system. The performance of the system is gauged through

Chapter 6

residual ranging error CDF and outage probability. In addition, the proposed FIS is compared with [12], and results show that the FIS is more effective than [12] in reducing errors and delay in estimating the error in the condition. Moreover, the system designing consider errors in LOS conditions due to MPP which is a novel approach. The proposed system is intended for indoor tracking and navigation where the probability of NLOS occurrence for more than one AN-TN link is high, and there is a critical need for precision localization in which accuracy is high while the delay in position estimation is low.

6.2. Feature Research Direction

In this dissertation, the proposed techniques namely classification and fuzzy based ranging error correction are validated in an offline mode. It is interesting that procedure (particularly fuzzy inference system) would be converted into embedded compatible codes for real-time implementation. In addition, sensor fusion technique would be considered in which inertial measurement sensing parameters are fused with fuzzy mitigated ranges. The technique would be implemented using an extended Kalman filter for enhancing tracking control.

REFERENCES

- [1] Decawave. www.decawave.com.
- [2] C. Röhrig and M. Müller, "Indoor location tracking in non-line-of-sight environments using a IEEE 802.15. 4a wireless network," in *IROS*, 2009, pp. 552-557.
- [3] H. Wymeersch, S. Marano, W. M. Gifford, and M. Z. Win, "A machine learning approach to ranging error mitigation for UWB localization," *IEEE Transactions on Communications*, vol. 60, pp. 1719-1728, 2012.
- [4] W. Liu and X. Huang, "Analysis of energy detection receiver for TOA estimation in IR UWB ranging and a novel TOA estimation approach," *Journal of Electromagnetic Waves and Applications*, vol. 28, pp. 49-63, 2014.
- [5] I. Guvenc, C.-C. Chong, and F. Watanabe, "NLOS identification and mitigation for UWB localization systems," in *Wireless Communications and Networking Conference, 2007. WCNC 2007. IEEE*, 2007, pp. 1571-1576.
- [6] B. Silva and G. P. Hancke, "IR-UWB-based non-line-of-sight identification in harsh environments: Principles and challenges," *IEEE Transactions on Industrial Informatics*, vol. 12, pp. 1188-1195, 2016.
- [7] W. M. G. S. Marano, H. Wymeersch, M. Z. Win, "NLOS Identification and mitigation for Localization based on UWB experimental data," *IEEE Journal on selected areas in communications*, vol. 28, pp. 1026-1035, Sep. 2010 2010.
- [8] S. M. Henk Wymeersch and a. M. Z. W. Wesley M. Gifford, "A Machine Learning Approach to Ranging Error Mitigation for UWB Localization," *IEEE TRANSACTIONS ON COMMUNICATIONS*, vol. 60, NO. 6, JUNE 2012.
- [9] L. Z. S. Tian, G. Li, "A support vector data description approach to NLOS identification in UWB positioning," *Mathematical Problems in Engineering*, vol. 2014, pp. 1-6, 2014.
- [10] X. L. Bo You, Xudong Zhao, Yijun Gao, "A Novel Robust Algorithm Attenuating Non-Line-of-Sight Errors in Indoor Localization," presented at the 2015 IEEE International Conference on Communication Software and Networks (ICCSN), 2015.
- [11] M. Kolakowski and J. Modelski, "First path component power based NLOS mitigation in UWB positioning system," in *Telecommunication Forum (TELFOR), 2017 25th*, 2017, pp. 1-4.
- [12] K. Y. a. Y. L. Kai Wen, "NLOS Identification and Compensation for UWB Ranging Based on Obstruction Classification," presented at the 25th European Signal Processing Conference (EUSIPCO), 2017
- [13] D. Dardari, P. Closas, and P. M. Djuric, "Indoor Tracking: Theory, Methods, and Technologies," *IEEE Trans. Vehicular Technology*, vol. 64, pp. 1263-1278, 2015.
- [14] M. M. Atia, S. Liu, H. Nematallah, T. B. Karamat, and A. Noureldin, "Integrated indoor navigation system for ground vehicles with automatic 3-D alignment and position initialization," *IEEE Transactions on Vehicular Technology*, vol. 64, pp. 1279-1292, 2015.
- [15] C. Fuchs, N. Aschenbruck, P. Martini, and M. Wieneke, "Indoor tracking for mission critical scenarios: A survey," *Pervasive and Mobile Computing*, vol. 7, pp. 1-15, 2011.
- [16] R. Bharadwaj, C. Parini, and A. Alomainy, "Indoor tracking of human movements using UWB technology for motion capture," in *Antennas and Propagation (EuCAP), 2014 8th European Conference on*, 2014, pp. 2097-2099.

- [17] M. J. Segura, V. A. Mut, and H. D. Patiño, "Mobile robot self-localization system using IR-UWB sensor in indoor environments," in *Robotic and Sensors Environments, 2009. ROSE 2009. IEEE International Workshop on*, 2009, pp. 29-34.
- [18] S. Marano, W. M. Gifford, H. Wymeersch, and M. Z. Win, "NLOS identification and mitigation for localization based on UWB experimental data," *IEEE Journal on Selected Areas in Communications*, vol. 28, 2010.
- [19] Y. Ham, K. K. Han, J. J. Lin, and M. Golparvar-Fard, "Visual monitoring of civil infrastructure systems via camera-equipped Unmanned Aerial Vehicles (UAVs): a review of related works," *Visualization in Engineering*, vol. 4, p. 1, 2016.
- [20] L. Aprville, T. Tanzi, and J.-L. Dugelay, "Autonomous drones for assisting rescue services within the context of natural disasters," in *General Assembly and Scientific Symposium (URSI GASS), 2014 XXXIth URSI*, 2014, pp. 1-4.
- [21] G. Han, J. Jiang, C. Zhang, T. Q. Duong, M. Guizani, and G. K. Karagiannidis, "A Survey on Mobile Anchor Node Assisted Localization in Wireless Sensor Networks," *IEEE Communications Surveys and Tutorials*, vol. 18, pp. 2220-2243, 2016.
- [22] Y. Gu, A. Lo, and I. Niemegeers, "A survey of indoor positioning systems for wireless personal networks," *IEEE Communications surveys & tutorials*, vol. 11, pp. 13-32, 2009.
- [23] J. B. Andersen, T. S. Rappaport, and S. Yoshida, "Propagation measurements and models for wireless communications channels," *IEEE Communications Magazine*, vol. 33, pp. 42-49, 1995.
- [24] H. Nurminen, T. Ardesiri, R. Piché, and F. Gustafsson, "A NLOS-robust TOA positioning filter based on a skew-t measurement noise model," in *Indoor Positioning and Indoor Navigation (IPIN), 2015 International Conference on*, 2015, pp. 1-7.
- [25] Z. Xiao, H. Wen, A. Markham, N. Trigoni, P. Blunsom, and J. Frolik, "Non-line-of-sight identification and mitigation using received signal strength," *IEEE Transactions on Wireless Communications*, vol. 14, pp. 1689-1702, 2015.
- [26] S. W. J. Karedal, P. Almers, F. Tufvesson, A. F. Molisch, "A measurement-based statistical model for industrial ultra-wideband channels," *IEEE Transactions on Wireless Communications*, vol. 6, pp. 3028-3037, Aug. 2007 2007.
- [27] K. Langendoen and N. Reijers, "Distributed localization in wireless sensor networks: a quantitative comparison," *Computer networks*, vol. 43, pp. 499-518, 2003.
- [28] I. F. Akyildiz, T. Melodia, and K. R. Chowdury, "Wireless multimedia sensor networks: A survey," *IEEE Wireless Communications*, vol. 14, 2007.
- [29] S. M. H. Wymeersch, W. M. Gifford, M. Z. Win, "A machine learning approach to ranging error mitigation for UWB localization," *IEEE Transactions on Communications*, vol. 60, June 2012 2012.
- [30] Q. Wang, I. Balasingham, M. Zhang, and X. Huang, "Improving RSS-based ranging in LOS-NLOS scenario using GMMs," *IEEE Communications Letters*, vol. 15, pp. 1065-1067, 2011.
- [31] K. Kaemarungsi and P. Krishnamurthy, "Properties of indoor received signal strength for WLAN location fingerprinting," in *Mobile and Ubiquitous Systems: Networking and Services, 2004. MOBIQUITOUS 2004. The First Annual International Conference on*, 2004, pp. 14-23.
- [32] M. Sugano, T. Kawazoe, Y. Ohta, and M. Murata, "Indoor Localization System using RSSI Measurement of Wireless Sensor Network based on ZigBee Standard," in *Wireless and Optical Communications*, 2006, pp. 1-6.
- [33] H. Liu, H. Darabi, P. Banerjee, and J. Liu, "Survey of wireless indoor positioning techniques and systems," *IEEE Transactions on Systems, Man, and Cybernetics, Part C (Applications and Reviews)*, vol. 37, pp. 1067-1080, 2007.
- [34] Z.-A. Deng, Y. Hu, J. Yu, and Z. Na, "Extended kalman filter for real time indoor localization by fusing WiFi and smartphone inertial sensors," *Micromachines*, vol. 6, pp. 523-543, 2015.

- [35] S. Yousefi, X.-W. Chang, and B. Champagne, "Mobile localization in non-line-of-sight using constrained square-root unscented Kalman filter," *IEEE Transactions on Vehicular Technology*, vol. 64, pp. 2071-2083, 2015.
- [36] S. He and S.-H. G. Chan, "Wi-Fi fingerprint-based indoor positioning: Recent advances and comparisons," *IEEE Communications Surveys & Tutorials*, vol. 18, pp. 466-490, 2016.
- [37] B. Soret, K. I. Pedersen, N. T. Jørgensen, and V. Fernández-López, "Interference coordination for dense wireless networks," *IEEE Communications Magazine*, vol. 53, pp. 102-109, 2015.
- [38] V. Nguyen, A. Q. Javaid, and M. A. Weitnauer, "Harmonic Path (HAPA) algorithm for non-contact vital signs monitoring with IR-UWB radar," in *Biomedical Circuits and Systems Conference (BioCAS), 2013 IEEE*, 2013, pp. 146-149.
- [39] K. György, A. Kelemen, and L. Dávid, "Unscented Kalman filters and Particle Filter methods for nonlinear state estimation," *Procedia Technology*, vol. 12, pp. 65-74, 2014.
- [40] K. Gururaj, A. K. Rajendra, Y. Song, C. L. Law, and G. Cai, "Real-time identification of NLOS range measurements for enhanced UWB localization," in *Indoor Positioning and Indoor Navigation (IPIN), 2017 International Conference on*, 2017, pp. 1-7.
- [41] M. J. Patyra, J. L. Grantner, and K. Koster, "Digital fuzzy logic controller: design and implementation," *IEEE Transactions on Fuzzy Systems*, vol. 4, pp. 439-459, 1996.
- [42] A. W. Tsui, Y.-H. Chuang, and H.-H. Chu, "Unsupervised learning for solving RSS hardware variance problem in WiFi localization," *Mobile Networks and Applications*, vol. 14, pp. 677-691, 2009.
- [43] F. Palumbo, P. Barsocchi, S. Chessa, and J. C. Augusto, "A stigmergic approach to indoor localization using bluetooth low energy beacons," in *2015 12th IEEE International Conference on Advanced Video and Signal Based Surveillance (AVSS)*, 2015, pp. 1-6.
- [44] P. Kumar, L. Reddy, and S. Varma, "Distance measurement and error estimation scheme for RSSI based localization in Wireless Sensor Networks," in *Wireless Communication and Sensor Networks (WCSN), 2009 Fifth IEEE Conference on*, 2009, pp. 1-4.
- [45] H. Mazar, *Radio Spectrum Management: Policies, Regulations and Techniques*: John Wiley & Sons, 2016.
- [46] J. Shirahama and T. Ohtsuki, "RSS-based localization in environments with different path loss exponent for each link," in *Vehicular technology conference, 2008. VTC spring 2008. IEEE*, 2008, pp. 1509-1513.
- [47] I. Guvenc and Z. Sahinoglu, "Threshold-based TOA estimation for impulse radio UWB systems," in *Ultra-Wideband, 2005. ICU 2005. 2005 IEEE International Conference on*, 2005, pp. 420-425.
- [48] !!! INVALID CITATION !!!
- [49] Y.-T. Chan, W.-Y. Tsui, H.-C. So, and P.-c. Ching, "Time-of-arrival based localization under NLOS conditions," *IEEE Trans. Vehicular Technology*, vol. 55, pp. 17-24, 2006.
- [50] H.-y. WANG, Y.-f. LAN, B.-n. PEI, and Y.-f. FANG, "A location algorithm based on TDOA under NLOS environment [J]," *Computer Simulation*, vol. 9, p. 032, 2007.
- [51] Y. Zhou, C. L. Law, Y. L. Guan, and F. Chin, "Indoor elliptical localization based on asynchronous UWB range measurement," *IEEE Transactions on Instrumentation and Measurement*, vol. 60, pp. 248-257, 2011.
- [52] Y. Xu, Y. S. Shmaliy, Y. Li, and X. Chen, "UWB-based indoor human localization with time-delayed data using EFIR filtering," *IEEE Access*, vol. 5, pp. 16676-16683, 2017.
- [53] A. Lazaro, D. Girbau, and R. Villarino, "Analysis of vital signs monitoring using an IR-UWB radar," *Progress In Electromagnetics Research*, vol. 100, pp. 265-284, 2010.
- [54] M. Verhelst, N. Van Helleputte, G. Gielen, and W. Dehaene, "A reconfigurable, 0.13 μm CMOS 110pJ/pulse, fully integrated IR-UWB receiver for communication and sub-cm ranging," in *Solid-*

- State Circuits Conference-Digest of Technical Papers, 2009. ISSCC 2009. IEEE International*, 2009, pp. 250-251,251 a.
- [55] J. R. Fernandes and D. D. Wentzloff, "Recent advances in IR-UWB transceivers: An overview," in *ISCAS*, 2010, pp. 3284-3287.
 - [56] A. F. Molisch, K. Balakrishnan, D. Cassioli, C.-C. Chong, S. Emami, A. Fort, *et al.*, "IEEE 802.15. 4a channel model-final report," *IEEE P802*, vol. 15, p. 0662, 2004.
 - [57] J. Padgett, "Guide to bluetooth security," *NIST Special Publication*, vol. 800, p. 121, 2017.
 - [58] A. Baniukevic, C. S. Jensen, and H. Lu, "Hybrid indoor positioning with wi-fi and bluetooth: Architecture and performance," in *Mobile Data Management (MDM), 2013 IEEE 14th International Conference on*, 2013, pp. 207-216.
 - [59] Z. Specification, "ZigBee Alliance," *ZigBee Document 053474r06, Version*, vol. 1, 2006.
 - [60] V. K. Chillara, Y.-H. Liu, B. Wang, A. Ba, M. Vidojkovic, K. Philips, *et al.*, "9.8 An 860 μ W 2.1-to-2.7 GHz all-digital PLL-based frequency modulator with a DTC-assisted snapshot TDC for WPAN (Bluetooth Smart and ZigBee) applications," in *Solid-State Circuits Conference Digest of Technical Papers (ISSCC), 2014 IEEE International*, 2014, pp. 172-173.
 - [61] D. He, "The zigbee wireless sensor network in medical care applications," in *Computer, Mechatronics, Control and Electronic Engineering (CMCE), 2010 International Conference on*, 2010, pp. 497-500.
 - [62] C.-N. Huang and C.-T. Chan, "ZigBee-based indoor location system by k-nearest neighbor algorithm with weighted RSSI," *Procedia Computer Science*, vol. 5, pp. 58-65, 2011.
 - [63] J. Larranaga, L. Mugira, J.-M. Lopez-Garde, and J.-I. Vazquez, "An environment adaptive ZigBee-based indoor positioning algorithm," in *Indoor Positioning and Indoor Navigation (IPIN), 2010 International Conference on*, 2010, pp. 1-8.
 - [64] W. Murphy and W. Hereman, "Determination of a position in three dimensions using trilateration and approximate distances," *Department of Mathematical and Computer Sciences, Colorado School of Mines, Golden, Colorado, MCS-95*, vol. 7, p. 19, 1995.
 - [65] S. Yousefi, X.-W. Chang, and B. Champagne, "An Improved Extended Kalman Filter for Localization of a Mobile Node with NLOS Anchors," in *Proceedings of the Ninth International Conference on Wireless and Mobile Communications (ICWMC)*, 2013, pp. 25-30.
 - [66] D. Kakkar, P. Karbownik, T. Nowak, N. Franke, and R. Galas, "Analysis of bayesian filters for position estimation in ultra-wideband localization systems," in *The European Navigation Conference, Vienna*, 2013.
 - [67] Z. Daixian and Y. Kechu, "Particle filter localization in underground mines using UWB ranging," in *Intelligent Computation Technology and Automation (ICICTA), 2011 International Conference on*, 2011, pp. 645-648.
 - [68] B. Sobhani, E. Paolini, M. Mazzotti, A. Giorgetti, and M. Chiani, "Multiple target tracking with particle filtering in UWB radar sensor networks," in *Localization and GNSS (ICL-GNSS), 2015 International Conference on*, 2015, pp. 1-6.
 - [69] Y. Yang, Y. Zhao, and M. Kyas, "A statistics-based least squares (SLS) method for non-line-of-sight error of indoor localization," in *Wireless Communications and Networking Conference (WCNC), 2013 IEEE*, 2013, pp. 2299-2304.
 - [70] W. Xu, Z. Wang, and S. A. Zekavat, "An introduction to NLOS identification and localization," *Handbook of Position Location: Theory, Practice, and Advances*, pp. 523-555, 2011.
 - [71] L. Luoh, "ZigBee-based intelligent indoor positioning system soft computing," *Soft Computing*, vol. 18, pp. 443-456, 2014.

- [72] A. H. Sayed, A. Tarighat, and N. Khajehnouri, "Network-based wireless location: challenges faced in developing techniques for accurate wireless location information," *IEEE signal processing magazine*, vol. 22, pp. 24-40, 2005.
- [73] P. Melin and O. Castillo, "A review on type-2 fuzzy logic applications in clustering, classification and pattern recognition," *Applied soft computing*, vol. 21, pp. 568-577, 2014.
- [74] T. Garcia-Valverde, A. Garcia-Sola, H. Hagra, J. A. Dooley, V. Callaghan, and J. A. Botia, "A fuzzy logic-based system for indoor localization using WiFi in ambient intelligent environments," *IEEE Transactions on Fuzzy Systems*, vol. 21, pp. 702-718, 2013.
- [75] P. Torteeka and X. Chundi, "Indoor positioning based on Wi-Fi fingerprint technique using fuzzy K-nearest neighbor," in *Proc. 11 th International Bhurban Conference on Applied Sciences & Technology (IBCAST)*, 2014, pp. 461-465.
- [76] A. Celikyilmaz and I. B. Turksen, "Modeling uncertainty with fuzzy logic," *Studies in fuzziness and soft computing*, vol. 240, pp. 149-215, 2009.
- [77] H. Bustince, F. Herrera, and J. Montero, *Fuzzy Sets and Their Extensions: Representation, Aggregation and Models: Intelligent Systems from Decision Making to Data Mining, Web Intelligence and Computer Vision* vol. 220: Springer, 2007.



Sunil Kumar <kumar11d@uwindsor.ca>

Permission to use papers in my dissertation

University of Windsor Mail - Permission to use papers in my dissertation
<https://mail.google.com/mail/u/0?ik=bd6a6a3e35&view=pt&search=all...>

2 messages

Sunil Kumar <kumar11d@uwindsor.ca> Wed, Oct 10, 2018 at 11:40 AM
To: Kemal Tepe <ktepe@uwindsor.ca>

Dear Dr. Tepe,

Please can I have your permission for use the following papers in my dissertation:

1. Empirical Based Ranging Error Mitigation in IR-UWB: A Fuzzy Approach
2. Received Signal Strength Based NLOS Classification & Mitigation in Ultra Wide Band Localization System
3. Accurate UWB and IMU based indoor localization for autonomous robots In chapters 3, 4 and 5.

Thanks & Regard,

Sunil Kumar Meghani

RA, GA, Ph.D. student

WiCIP,

University of Windsor

Kemal Tepe <ketepe@gmail.com> Wed, Oct 10, 2018 at 12:07 PM
Reply-To: ketepe@gmail.com
To: Sunil Kumar <kumar11d@uwindsor.ca>

I provide my permission to include these in your thesis.

[Quoted text hidden]

--Kemal Ertugrul Tepe ketepe@gmail.com

tepek@ieee.org

1 of 1 2018-10-12, 12:33 p.m.

Appendix A

University of Windsor Mail - Permission to use paper in my dissertation <https://mail.google.com/mail/u/0/?ik=bd6a6a3e35&view=pt&search=all...>



University
of Windsor

Sunil Kumar <kumar11d@uwindsor.ca>

Permission to use paper in my dissertation

2 messages

Sunil Kumar <kumar11d@uwindsor.ca>
To: Faroq Awin <awin@uwindsor.ca>

Wed, Oct 10, 2018 at 11:34 AM

Dear Dr. Awin,
Please can I have your permission for use the following paper in my
dissertation: Empirical Based Ranging Error Mitigation in IR-
UWB: A Fuzzy Approach
In chapters 3 and 5.
Thanks & Regard,
Sunil Kumar Meghani

RA, GA, Ph.D. student

WiCIP,

University of Windsor

Faroq Awin <awin@uwindsor.ca>
To: Sunil Kumar <kumar11d@uwindsor.ca>

Wed, Oct 10, 2018 at 11:35 AM

Yes, of course you can.

[Quoted text hidden]

1 of 1 2018-10-12, 12:38 p.m.

Appendix A

University of Windsor Mail - Permission to use paper in my dissertation <https://mail.google.com/mail/u/0/?ik=bd6a6a3e35&view=pt&search=all...>

Permission to use paper in my dissertation

2 messages

Sunil Kumar <kumar11d@uwindsor.ca>
To: Muhammad Asif <asif.arif@gmail.com>

Wed, Oct 10, 2018 at 11:32 AM

Dear Dr. Asif,
Please can I have your permission for use the following paper in my dissertation: Empirical Based Ranging Error Mitigation in IR-UWB: A Fuzzy Approach
In chapters 3 and 5.
Thanks & Regard,
Sunil Kumar Meghani

RA, GA, Ph.D. student

WiCIP,

University of Windsor



University
of Windsor

Sunil Kumar <kumar11d@uwindsor.ca>

Muhammad Asif <asif.arif@gmail.com> Wed, Oct 10, 2018 at 12:30 PM

To: Sunil Kumar <kumar11d@uwindsor.ca>

Yes, of course you can.

[Quoted text hidden]

1 of 1 2018-10-12, 12:42 p.m.

Appendix A

University of Windsor Mail - Permission to use paper in my dissertation <https://mail.google.com/mail/u/0/?ik=bd6a6a3e35&view=pt&search=all...>



Sunil Kumar <kumar11d@uwindsor.ca>

Permission to use paper in my dissertation

5 messages

Sunil Kumar <kumar11d@uwindsor.ca> Wed, Oct 10, 2018 at 11:47 AM

To: Brinda Tank <tankb@uwindsor.ca>, Alvin Marquez <marqueza@uwindsor.ca>, Sabbir Ahmed <Sabbir.Ahmed@uwindsor.ca >

Dear Colleagues,

Please can I have your permission for use the following paper in my dissertation: Accurate UWB and IMU based indoor localization for autonomous robots In chapters 3 and 5.

University of Windsor
Sabbir Ahmed
<Sabbir.Ahmed@uwindsor>
To: Sunil Meghani
<kumar11d@uwindsor.ca>

Wed, Oct 10, 2018 at 12:30 PM

Yes. No problem from my end.

Get [Outlook for Android](#)

From: Sunil Kumar
Sent: Wednesday, October 10, 11:47 AM
Subject: Permission to use paper in my dissertation
To: Brinda Tank, Alvin Marquez, Sabbir Ahmed

[Quoted text hidden]

Thanks & Regard,
Sunil Kumar Meghani

RA, GA, Ph.D. student

Appendix A

Sunil Kumar <kumar11d@uwindsor.ca>
To: alvinmarquez@hotmail.com

----- Forwarded message -----

From: **Sunil Kumar** <kumar11d@uwindsor.ca>
Date: Wed, Oct 10, 2018, 11:47 AM
Subject: Permission to use paper in my dissertation
[Quoted text hidden]
[Quoted text hidden]

WiCIP,

Alvin Marquez <alvinmarquez@hotmail.com> Thu, Oct 11, 2018 at 6:41 PM

1 of 2 2018-10-12, 12:45 p.m.

University of Windsor Mail - Permission to use paper in my dissertation <https://mail.google.com/mail/u/0/?ik=bd6a6a3e35&view=pt&search=all...>

Reply-To: alvinmarquez@hotmail.com
To: Sunil Kumar <kumar11d@uwindsor.ca>

Yes, you can.
[Quoted text hidden]

Brinda Tank <tankb@uwindsor.ca> Thu, Oct 11, 2018 at 8:09 PM
To: Sunil Kumar <kumar11d@uwindsor.ca>



Yes, you can.
[Quoted text hidden]

--

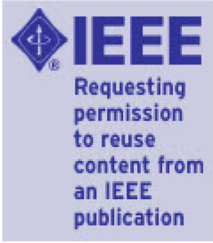
Thank you,
Brinda Tank

2 of 2 2018-10-12, 12:45 p.m.

Appendix A



[Home](#) [Create Account](#) [Help](#) 



Requesting permission to reuse content from an IEEE publication

Title	Accurate UWB and IMU based indoor localization for autonomous robots
Conference Proceedings	2017IEEE 30th Canadian Conference on Electrical and Computer Engineering (CCECE)
Author	A. Marquez, B. Tank, S.K. Meghani, S. Ahmed, K. Tepe
Publisher	IEEE

LOGIN
If you're a copyright.com user, you can login to RightsLink using your copyright.com credentials.
Already a **RightsLink user** want to [learn more?](#)

Rightslink® by Copyright Clearance Center <https://s100.copyright.com/AppDispatchServlet#formTop>

Date: April 2017

Copyright © 2017, IEEE

Thesis / Dissertation Reuse

The IEEE does not require individuals working on a thesis to obtain a formal reuse license, however, you may print out this statement to be used as a permission grant:

Requirements to be followed when using any portion (e.g., figure, graph, table, or textual material) of an IEEE copyrighted paper in a thesis:

- 1) In the case of textual material (e.g., using short quotes or referring to the work within these papers) users must give full credit to the original source (author, paper, publication) followed by the IEEE copyright line © 2011 IEEE.
- 2) In the case of illustrations or tabular material, we require that the copyright line © [Year of original publication] IEEE appear prominently with each reprinted figure and/or table.
- 3) If a substantial portion of the original paper is to be used, and if you are not the senior author, also obtain the senior author's approval.

Requirements to be followed when using an entire IEEE copyrighted paper in a thesis:

- 1) The following IEEE copyright/ credit notice should be placed prominently in the references: © [year of original publication] IEEE. Reprinted, with permission, from [author names, paper title, IEEE publication title, and month/year of publication]

Appendix A

- 2) Only the accepted version of an IEEE copyrighted paper can be used when posting the paper or your thesis on-line.
- 3) In placing the thesis on the author's university website, please display the following message in a prominent place on the website: In reference to IEEE copyrighted material which is used with permission in this thesis, the IEEE does not endorse any of [university/educational entity's name goes here]'s products or services. Internal or personal use of this material is permitted. If interested in reprinting/republishing IEEE copyrighted material for advertising or promotional purposes or for creating new collective works for resale or redistribution, please go to http://www.ieee.org/publications_standards/publications/rights/rights_link.html to learn how to obtain a License from RightsLink.

If applicable, University Microfilms and/or ProQuest Library, or the Archives of Canada may supply single copies of the dissertation.

BACK

CLOSE WINDOW

Copyright © 2018 [Copyright Clearance Center, Inc.](#) All Rights Reserved. [Privacy statement](#), [Terms and Conditions](#). Comments? We would like to hear from you. E-mail us at customercare@copyright.com

Name: Sunil Kumar Meghani.

Place of Birth: Karachi Pakistan.

Year of Birth: 1978.

Education:

BS (Electronic Engineering),

Sir Syed University of Engineering & Technology, Karachi Pakistan 2003.

MS (Modern Digital & Radio Frequency Wireless Communication),

University of Leeds, Leeds UK 2007.

Doctor of Philosophy (Electrical Engineering),

University of Windsor, Windsor ON Canada 2018.